Beam asymmetries of $\pi^0\eta$ photoproduction off protons

Qinghua HE (何庆华) for BGOegg Collaboration

July 13, 2025, Guilin

Outline

§ Why photoproduction?

§ BGOegg experiments

- Setup
- Selected physics topics

§ Beam asymmetries of $\pi^0\eta$ photoproduction

- Motivation
- Event selection
- Beam asymmetries

§ Discussion

§ Summary

Why photoproduction?

Hadron spectroscopy

-Still many quark models predicted resonances are missing for excited baryons (W>2 GeV)

-Mass ordering problem (e.g. N(1440) and N(1535))

GeV Photon probe is promising for searching these missing resonances

Meson photoproduction

$\gamma N \rightarrow N^{*} or \Delta^{*} \rightarrow$ mesons N for light baryon spectroscopy

-Short-lived resonances are overlapped with each other

BGOegg (E_{γ} =1.3-2.4 GeV)

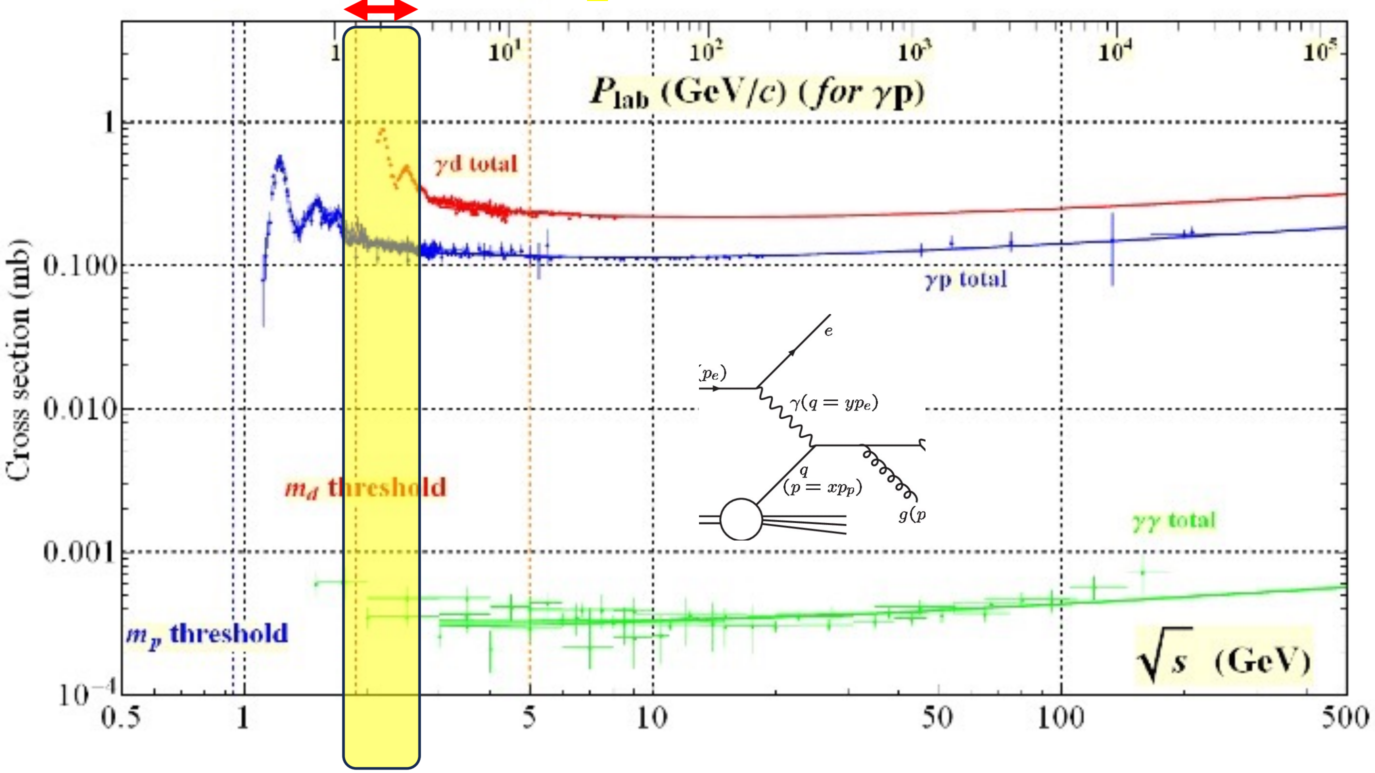

BGOegg experiment | setup

LEPS2/BGOegg Experiments

A large acceptance electromagnetic (EM) calorimeter BGOegg (Fig.1) was constructed at ELPH, Tohoku University. This calorimeter system has been transferred to the new laser Compton scattering beamline LEPS2 at SPring-8, where a 1.3-2.9 GeV photon beam with high linear polarization is available. The phase-1 experiments have started from 2014 April with the EM calorimeter BGOegg and the additional detectors for charged particles. We are now upgrading the experimental setup by covering most of the solid angles with EM calorimeters to start new data collection in the phase-2 experiments.

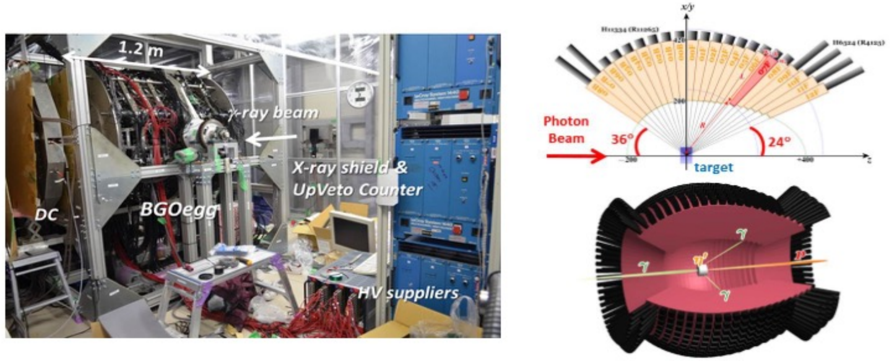

Fig.1 A picture of BGOegg inside the thermostatic booth (Left) and the drawings of BGOegg (Right).

Physics

experiments, we are planning to upgrade the detector setup as shown in Fig.3. Instead of using DC and RPC, the forward acceptance hole of the BGOegg calorimeter will be covered by additional EM calorimeters. We install the "Forward Gamma" detector, which consists of 252 PWO crystals, in the polar angle range of 3 to 16 degrees. We are also considering to cover the gap region between the BGOegg calorimeter and the Forward Gamma detector. This configuration will significantly reduce backgrounds in the direct measurement of η'-mass spectral shape using a nuleus target.

Status

The LEPS2/BGOegg experiments are carried out under the collaboration of ELPH (Tohoku University), RCNP (Osaka University), Nanjing University of Aeronautics and Astronautics, Kyoto University, KEK, RIKEN, JASRI (SPring-8), and many other institutes in the world. ELPH and RCNP cooperate the LEPS2 facility.

BGOegg experiment | setup

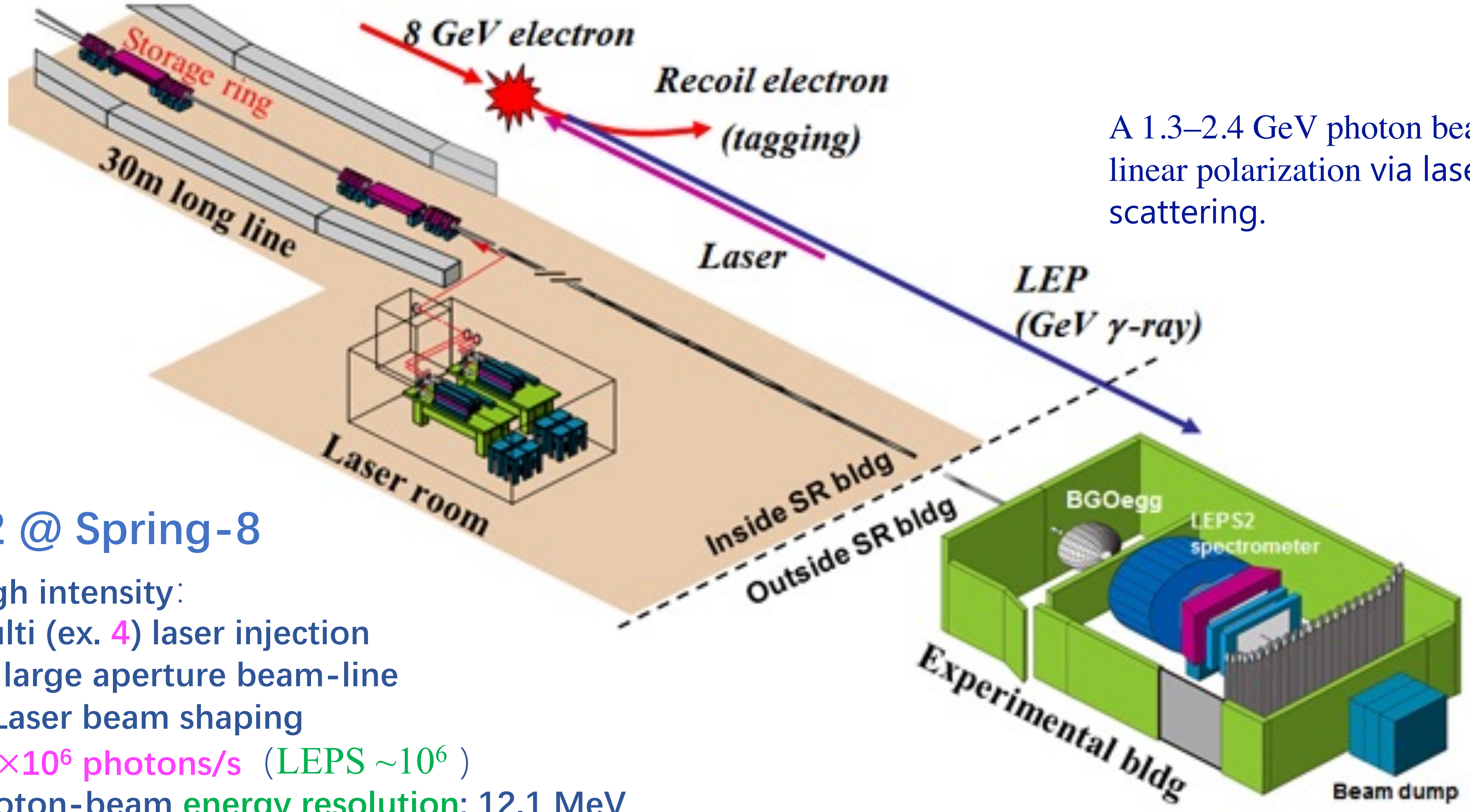

A 1.3–2.4 GeV photon beam with high linear polarization via laser Compton scattering.

LEPS2 @ Spring-8

High intensity:
Multi (ex. 4) laser injection
w/ large aperture beam-line
& Laser beam shaping
~5×10^6 photons/s (LEPS ~10^6)
Photon-beam energy resolution: 12.1 MeV

BGOegg experiment | setup

A 1.3–2.4 GeV photon beam with high linear polarization via laser Compton scattering

- LEPS2 beam is generated via laser Compton scattering.
- Other experimental facilities(CLAS, ELSA…) use coherent bremsstrahlung as a photon beam.

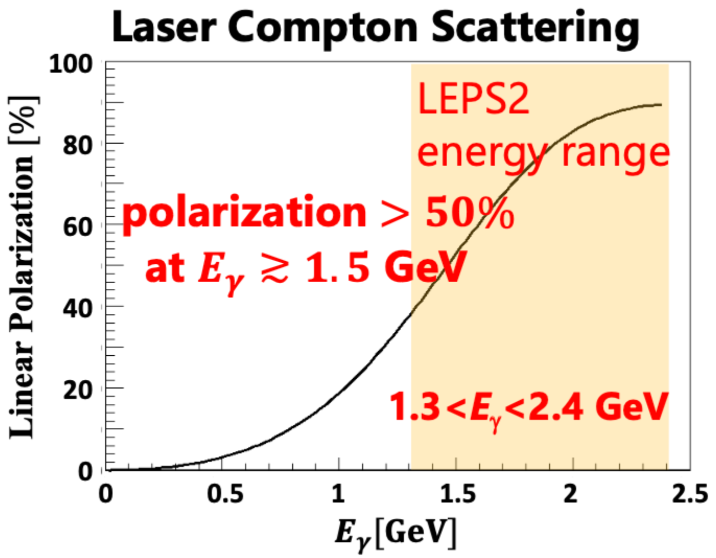

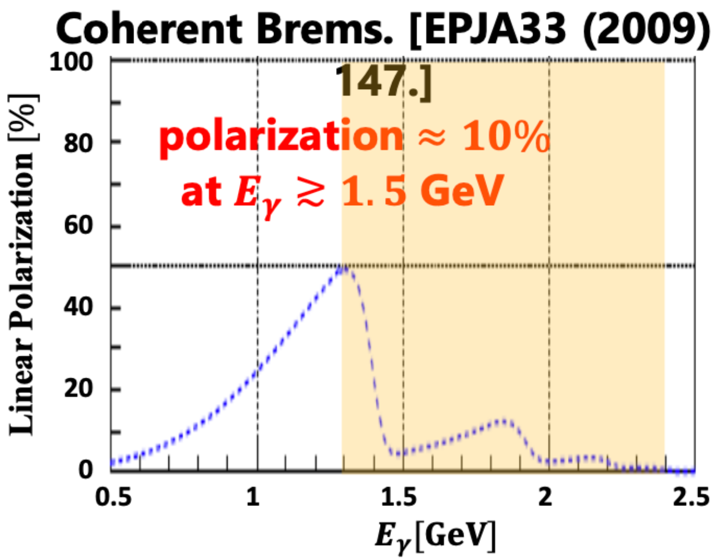

- LEPS2 beam polarization is **greater** than other experimental facilities at higher energies($E_\gamma \gtrsim 1.5$ **GeV**).

BGOegg experiment | setup

World leading energy resolution (carbon target)
π^0 mass resolution: 6.7 MeV/c^2;
η: 14.4 MeV/c^2)

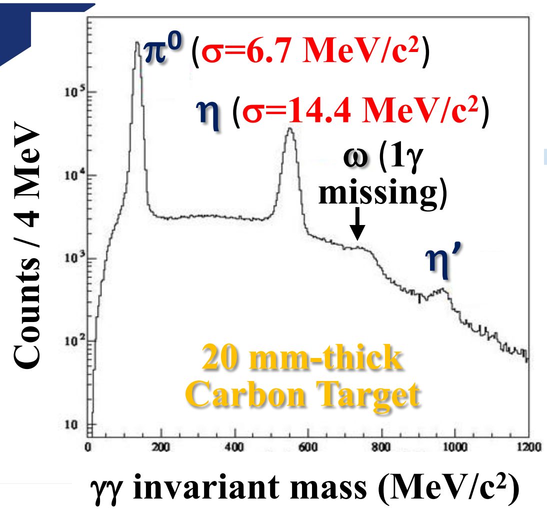

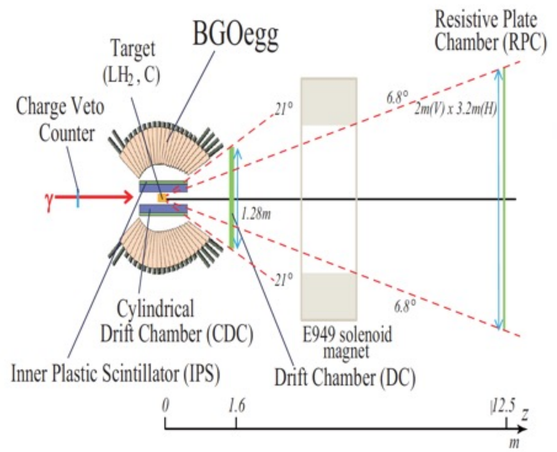

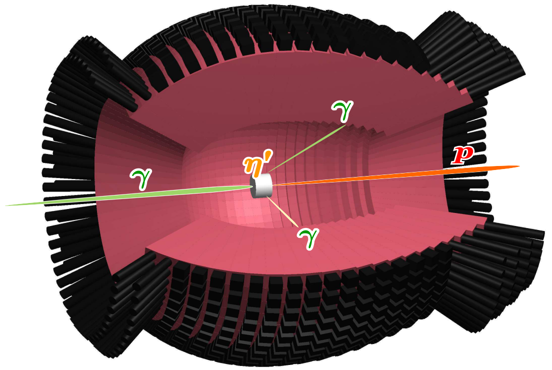

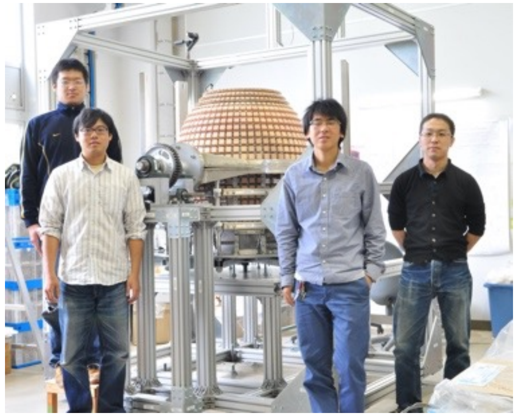

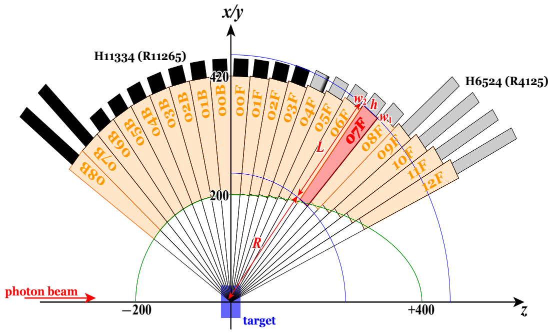

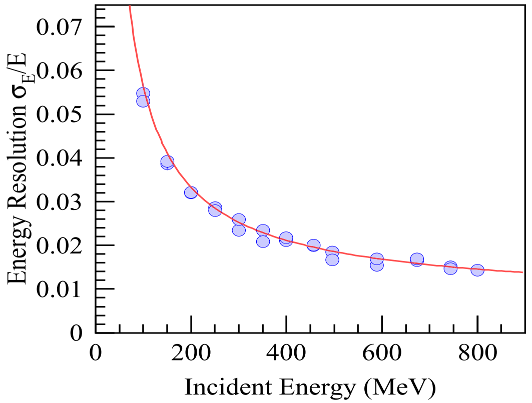

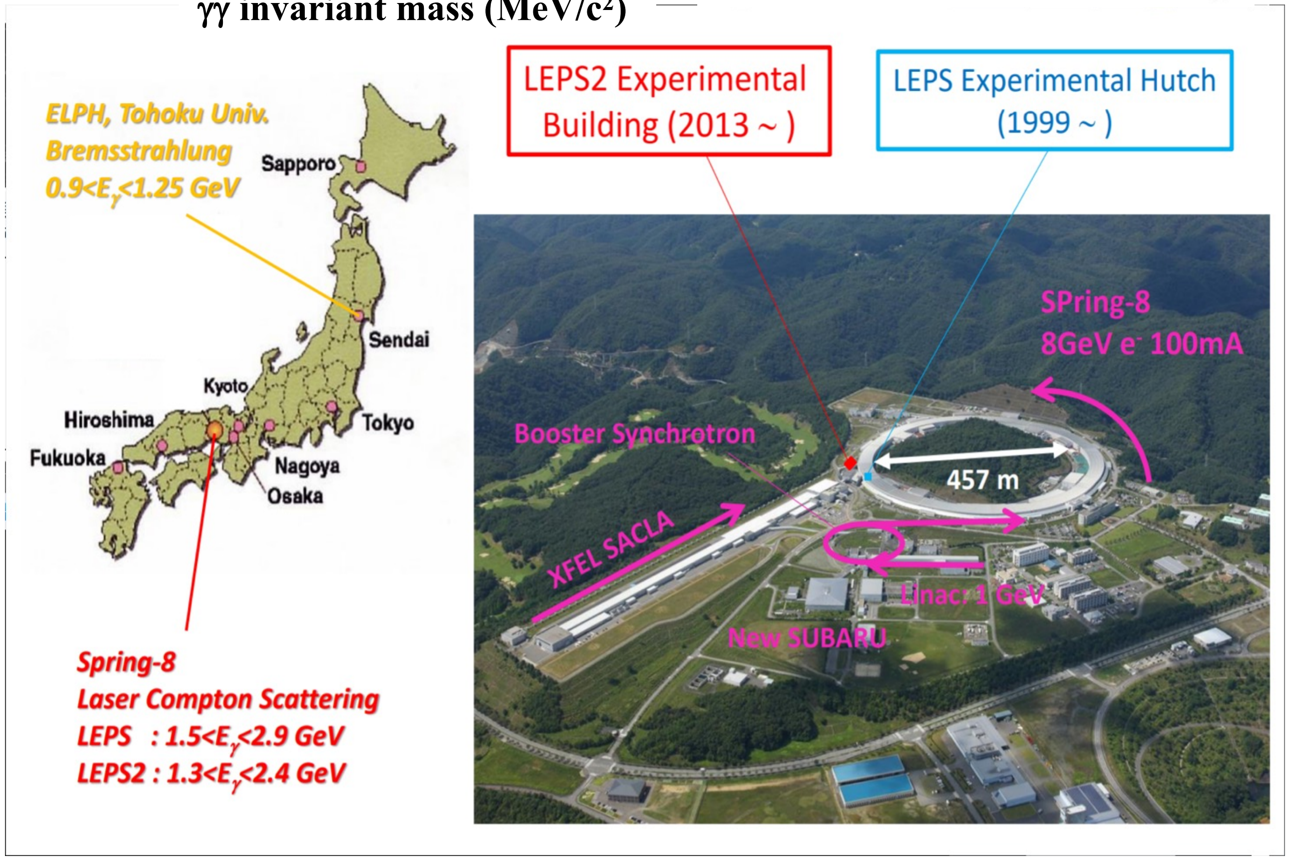

Target: LH2 (54mm) or Carbon (20 mm)

M. Miyabe, N. Muramatsu, H. Shimizu, et al., NIM paper in preparation.

BGOegg experiment | setup

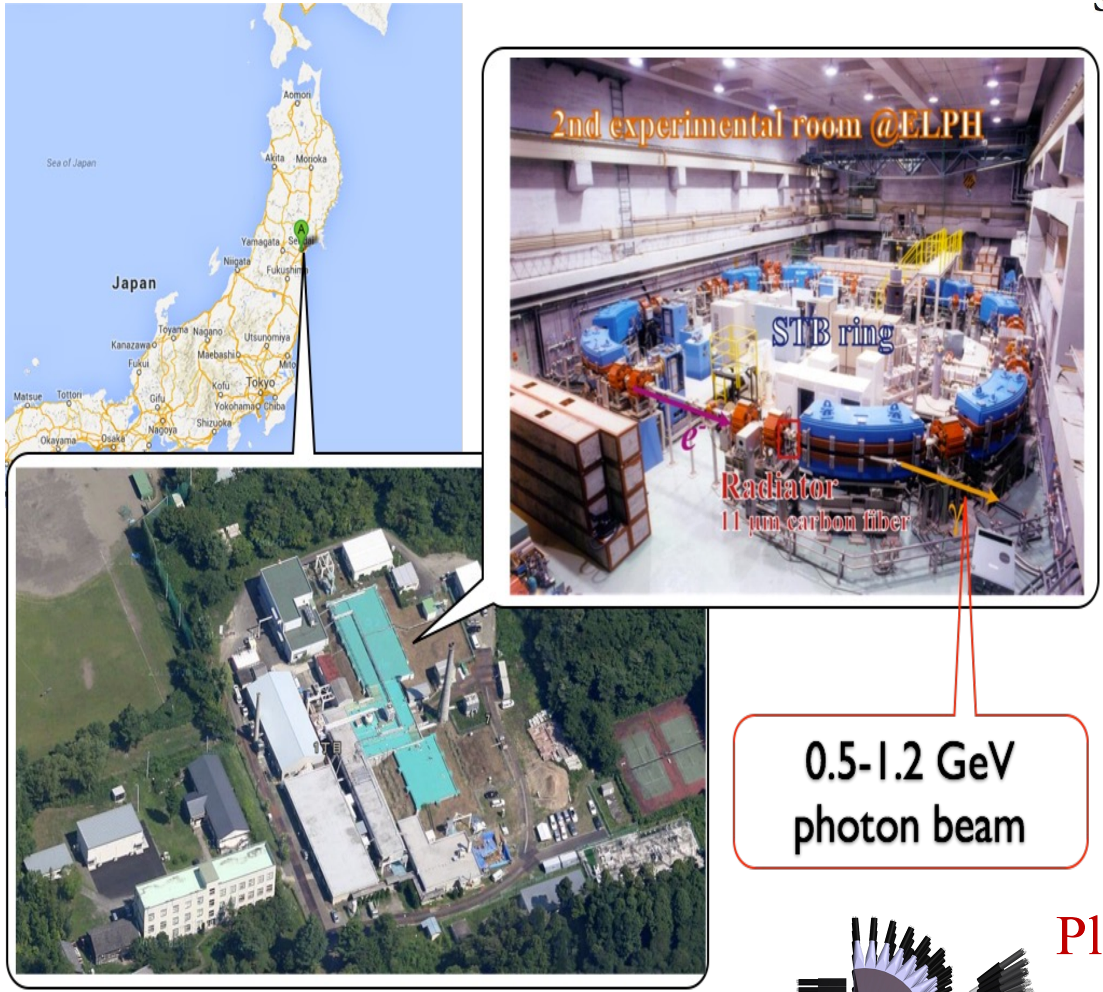

FOREST EM Calorimeter

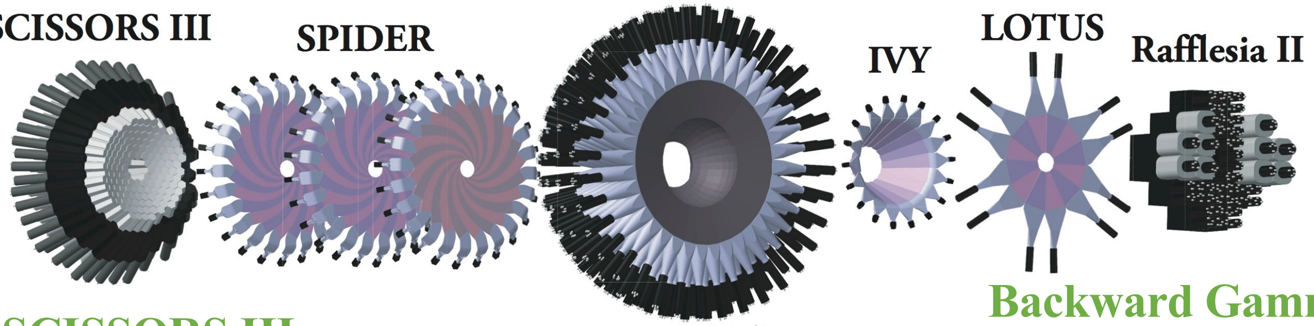

SCISSORS III
192 CsI; θ: 4°-24°, φ:full
Res. : 3% @ 1GeV

Backward Gamma
252 Lead/Scintillating fiber modules;
θ: 30°-100°, φ:full
Res. : 7% @ 1GeV

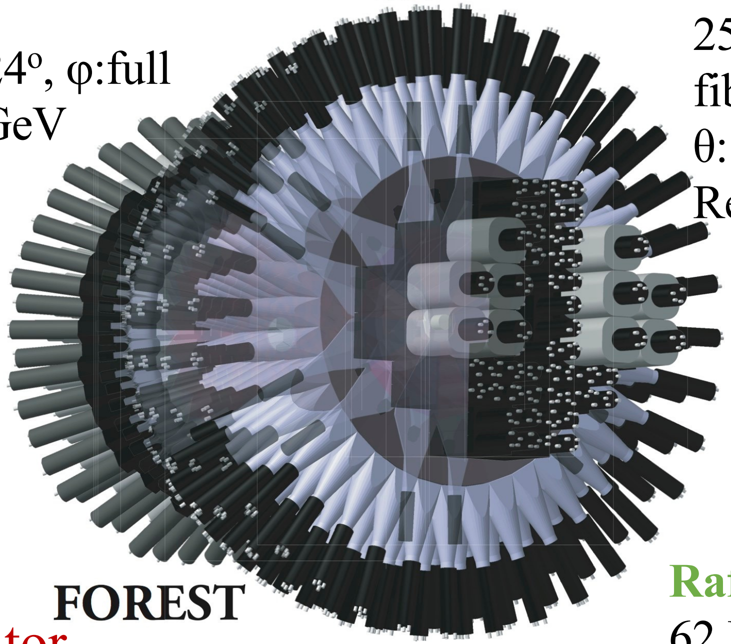

Rafflesia II
62 Lead Glass modules;
Res. : 5% @ 1GeV

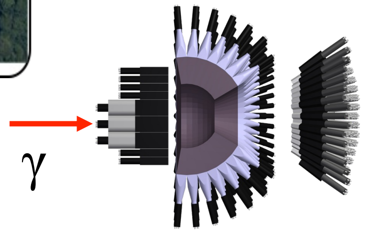

Plastic Scintillator

SPIDER (2 layers × 24 modules

IVY (18 modules)

LOTUS (12 modules)

BGOegg experiment | Selected physics topics

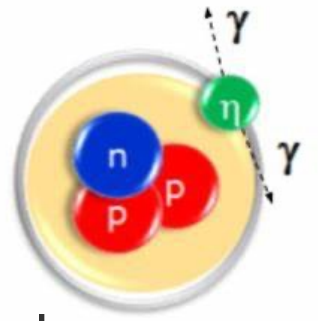

□ Search for η' mesic nuclei

- mass reduction of 80-150 MeV at nuclear density (partial restoration of chiral symmetry inside high-density condition)
- bound η' mesic nuclei in the C(γ,p)X reaction.

  Phys. Rev. Lett. 124, 202501 (2020)
- In-medium effect of the spectral shape of η’ (The width of η’ may change)
- The width of η’ may change
- Aaccurately measuring the spectrum of η’

□ Differential cross-section and beam asymmetry of the neutral mesons

The production of mesons from liquid hydrogen targets is suitable for investigating the excitation states of nucleons.

Phys. Rev. C 107, L042201 (2023)

SPring-8/SACLA Research Frontiers 2023 (2024)

□ $\pi^0\pi^0$ correlations

- measure the **space-time properties** of the particle emission source.

BGOegg experiment | Selected physics topics

Hadron mass origin

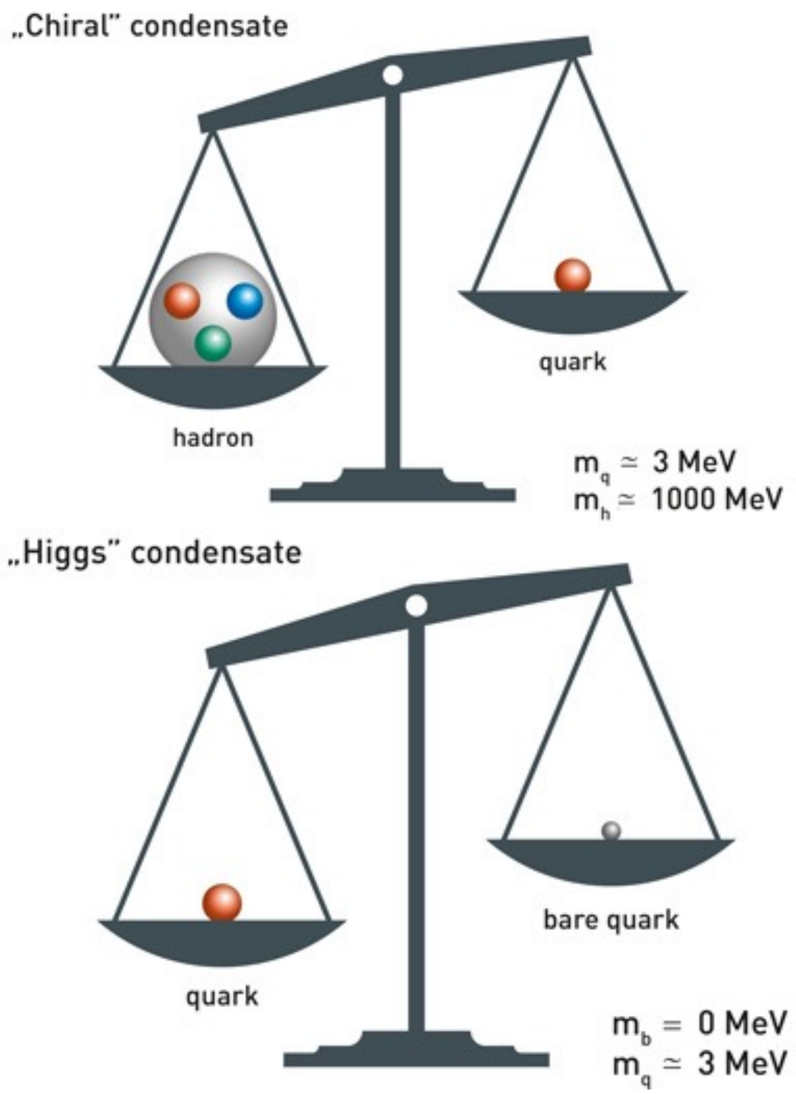

Yukawa coupling and Higgs particles explain the fundamental fermions masses， while the hadron mass is generated by the strong interaction in QCD。

Chiral symmetry breaking plays a key role to explain light hadrons masses

$U_A(1)$ symmetry breaking → $\eta'(985)$ exceptionally large mass
Mass gap between η' and η

Search for **the in-medium mass reduction of η′**（partial restoration of spontaneous chiral symmetry breaking may weaken the anomaly effect）

Nambu-Jona-Lasinio and linear sigma models containing an $U_A(1)$ symmetry breaking term → predict 150 and 80 MeV mass reduction

BGOegg experiment | Selected physics topics

Hadron mass origin

$$E_{\mathrm{ex}} - E_0^{\eta'} = MM[^{12}\mathrm{C}(\gamma, p_f)] - M_{^{11}\mathrm{B}} - M_{\eta'}$$

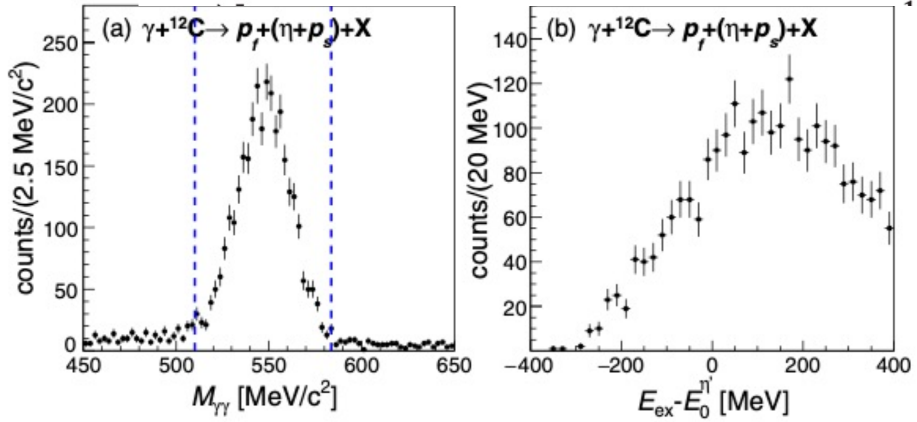

FIG. 1. (a) The 2γ invariant mass distribution around the η mass and (b) the excitation function of the $(\eta + p_s)$ coincidence data. The region in $\pm 2.5\sigma$ from the invariant mass peak is indicated by the blue-dashed lines.

- The mass reduction is described as an attractive potential for an η' meson in a nucleus
- **η'-nucleus bound states** can be formed.
- To search for η' -nucleus bound states, we used missing-mass spectroscopy of the $^{12}C(\gamma, p)$ reaction detecting decay products in coincidence.

We measured missing mass spectrum of the $^{12}\mathrm{C}(\gamma, p)$ reaction for the first time in coincidence with potential decay products from η' bound nuclei. We tagged an $(\eta + p)$ pair associated with the $\eta' N \to \eta N$ process in a nucleus. After applying kinematical selections to reduce backgrounds, no signal events were observed in the bound-state region. An upper limit of the signal cross section in the opening angle $\cos\theta_{\mathrm{lab}}^{\eta p} < -0.9$ was obtained to be 2.2 nb/sr at the 90% confidence level. It is compared with theoretical cross sections, whose normalization ambiguity is suppressed by measuring a quasifree η' production rate. Our results indicate a small branching fraction of the $\eta' N \to \eta N$ process and/or a shallow η'-nucleus potential.

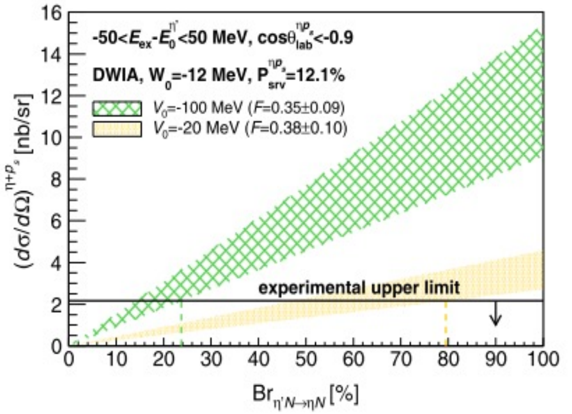

FIG. 4. The experimental upper limit of $(d\sigma/d\Omega)_{\mathrm{exp}}^{\eta+p_s}$ at the 90% confidence level, and $(d\sigma/d\Omega)_{\mathrm{theory}}^{\eta+p_s}$ as a function of $\mathrm{Br}_{\eta' N \to \eta N}$.

DOI: 10.1103/PhysRevLett.124.202501

Phys. Rev. Lett. **124**, 202501 (2020).

BGOegg experiment | Selected physics topics

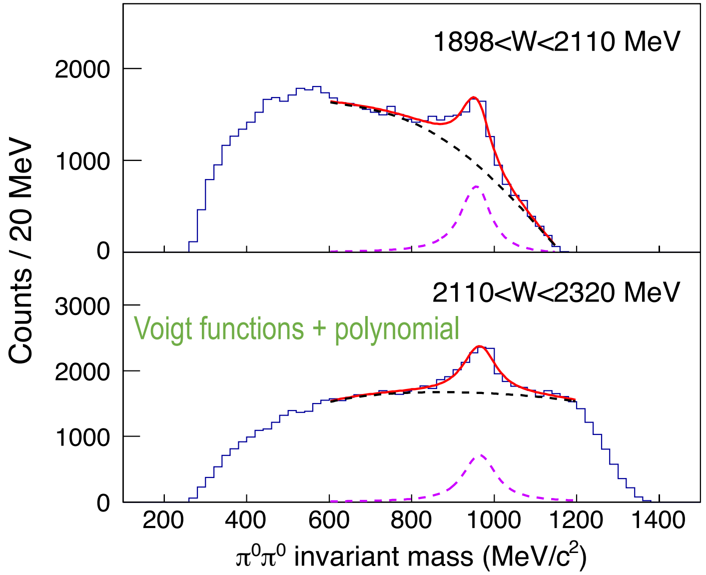

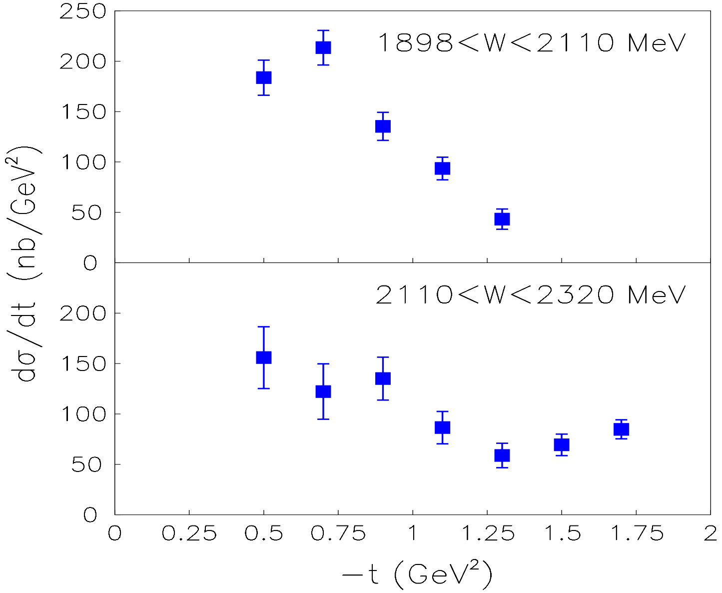

Beam asymmetries of $\gamma p \to f_0(980)p \to \pi^0\pi^0 p$ @E_γ = 1.3~2.4 GeV

$$N_{perp} = \int_{\pi/4}^{3/4\pi} \frac{d\sigma_0}{d\Omega}(1 - P_\gamma \Sigma \cos 2\Phi)d\Phi + \int_{5/4\pi}^{7/4\pi} \frac{d\sigma_0}{d\Omega}(1 - P_\gamma \Sigma \cos 2\Phi)d\Phi$$

$$N_{para} = \int_{-\pi/4}^{\pi/4} \frac{d\sigma_0}{d\Omega}(1 - P_\gamma \Sigma \cos 2\Phi)d\Phi + \int_{3/4\pi}^{5/4\pi} \frac{d\sigma_0}{d\Omega}(1 - P_\gamma \Sigma \cos 2\Phi)d\Phi,$$

$f_{int} = \pi/2$: correction factor for the integration over $\pi/2$ azimuthal angle ranges

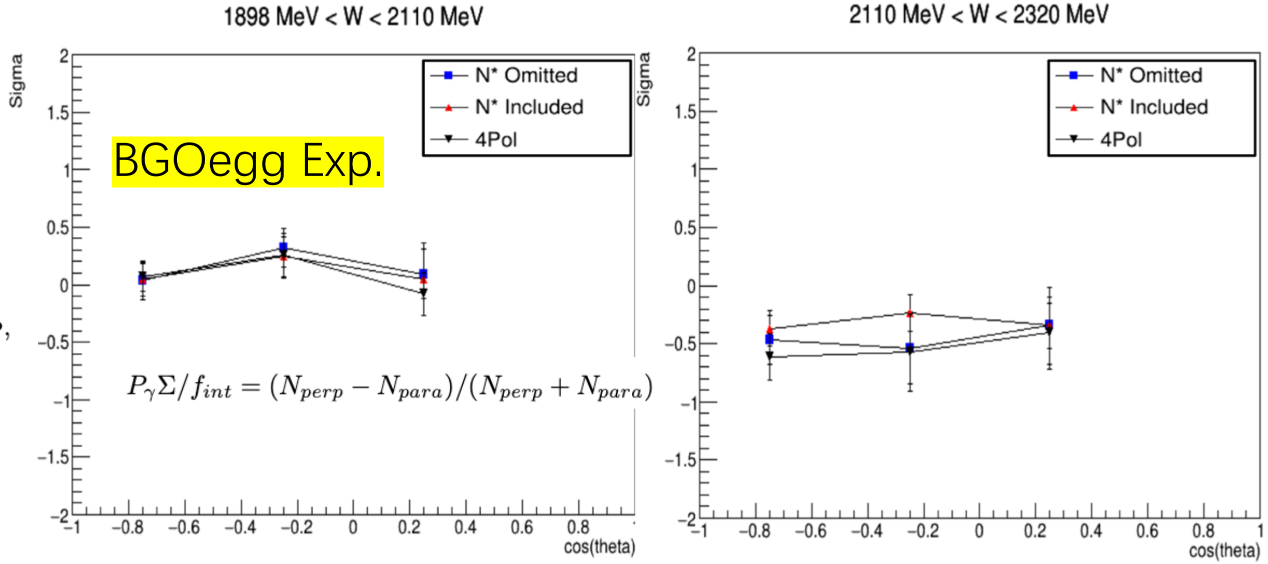

- The asymmetries Σs in the lower W bin are close to zero or slightly positive, while in the higher bin are negative values around -0.3, indicating the contribution of t-channel vector meson (natural parity) exchange in $f_0(980)$ photoproduction.
- At the higher energies, the deviation from $\Sigma = -1$ is seen possibly because of the unnatural parity contribution of axial-vector exchange [e.g., $b_1(1235)$] and re-scattering diagrams with two Reggeon exchange in addition to the contamination of s- and u-channel diagrams.
- The differential cross section $d\sigma/dt$ measured in a smaller $|-t|$ region is comparable to the theoretical prediction assuming a $q\bar{q}$ component in $f_0(980)$.

N. Muramatsu, S. K. Wang, Q. H. He , et al. (BGOegg), Phys. Rev. C 107, L042201 (2023)
Q. H. He, N. Muramatsu, SPring-8/SACLA Research Frontiers 2023 (2024)

BGOegg experiment | Selected physics topics

$\pi^0\pi^0$ correlations

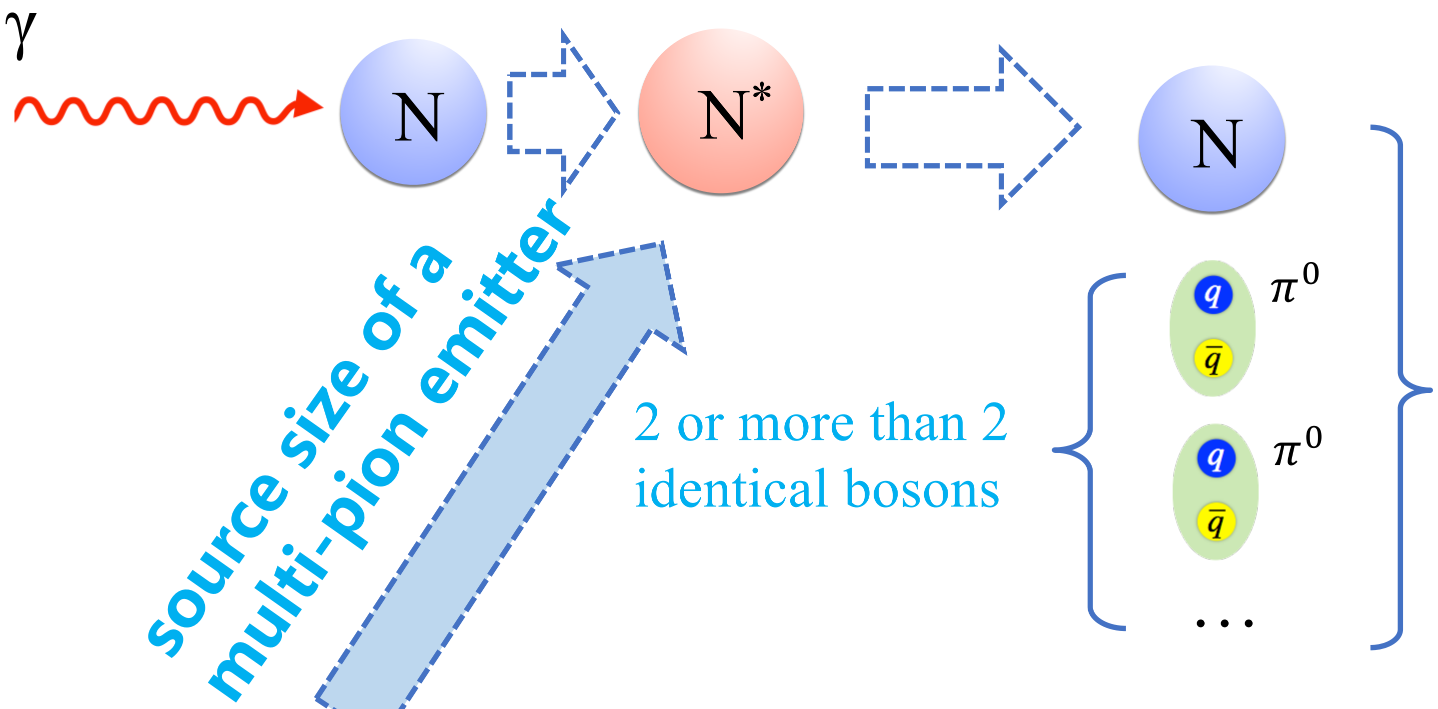

Intensity interference between identical particles (**HBT effects**) provides a tool to measure the space-time properties of the particle emission source.

$\gamma p \rightarrow \pi^0\pi^0 p$

1.3-2.4 GeV

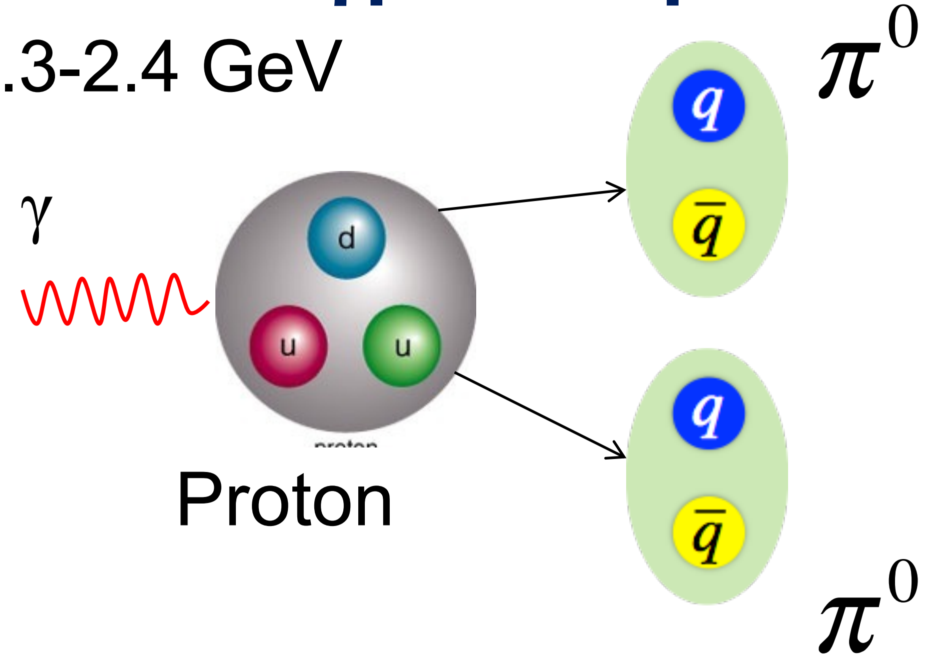

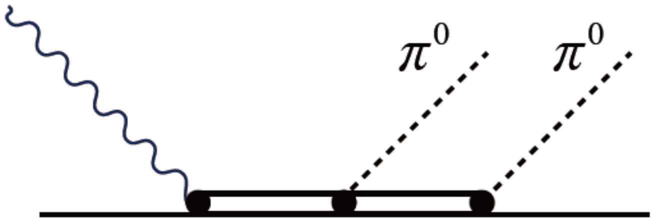

BGOegg experiment | Selected physics topics

$\gamma p \to \pi^0 \pi^0 p$

$\pi^0\pi^0$ correlations

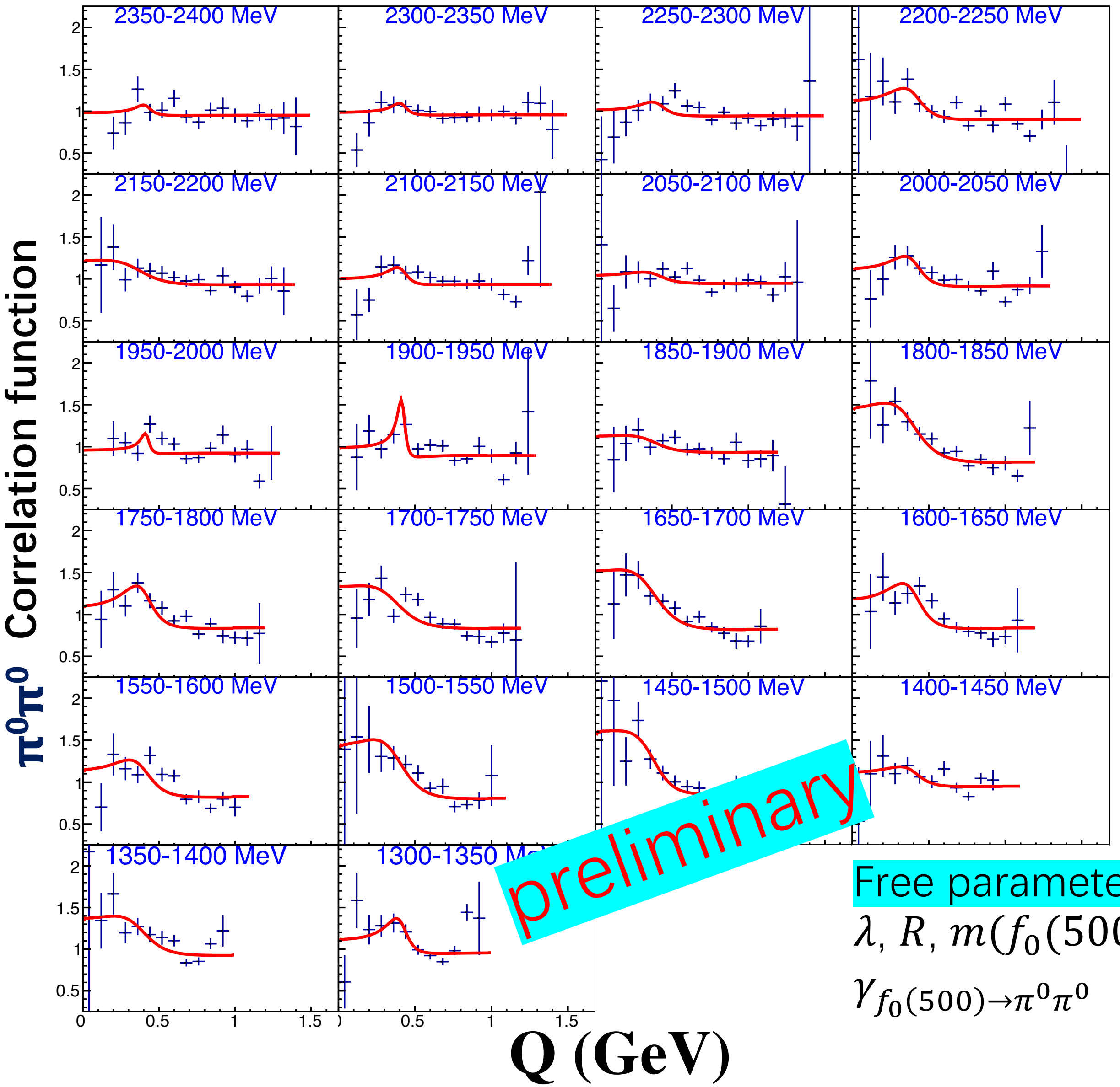

$$C_{Lednicky}(k^*) = 1 + \lambda e^{-4k^{*2}R^2} + \lambda\alpha\left[\left|\frac{f(k^*)}{R}\right|^2 + \frac{4\Re f(k^*)}{\sqrt{\pi}R}F_1(2k^*R) - \frac{2\Im f(k^*)}{R}F_2(2k^*R) + \Delta C\right]$$

$$F_1(z) = \int_0^z dx\,\frac{e^{x^2-z^2}}{z} \qquad F_2(z) = \frac{1-e^{-z^2}}{z}$$

$$f(k^*) = \frac{f_0(k^*) + f_1(k^*)}{2}$$

$$f_I(k^*) = \frac{\gamma_I}{m_I^2 - s - i(\gamma_I k^* + \gamma_I' k_I')}$$

$\Delta C = 0$ for the moment

* ALICE, PLB. 833 (2022) 137335.
* R. Molina, Z.W. Liu, L.S. Geng, E. Oset, EPJC. 84 (2024) 1–8.
* R. Molina, C.W. Xiao, W.H. Liang, E. Oset, ArXiv: 2310.12593

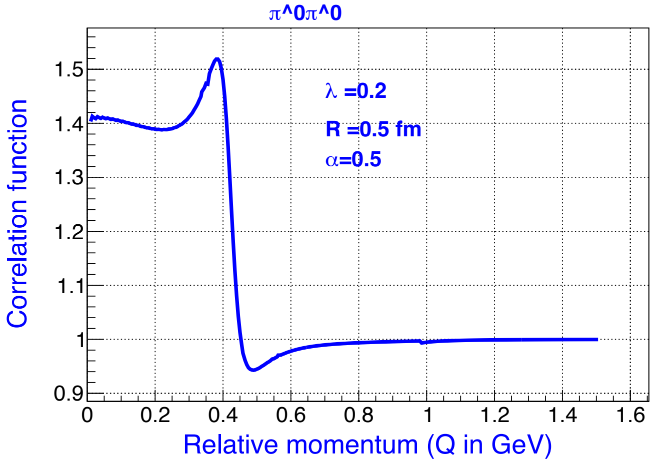

$f_0(500)$ mass	$\gamma_{\{f_0\to\pi^0\pi^0\}}$
0.5 GeV	0.18 GeV

$f_0(980)$ mass	$\gamma_{\{f_0\to\pi^0\pi^0\}}$	$\gamma_{\{f_0\to K\bar{K}\}}$
0.967	0.098	0.34

Free parameters:

λ, R, $m(f_0(500))$, $\gamma_{f_0(500)\to\pi^0\pi^0}$

Q. He, et al., Prog. Theor. Exp. Phys. **2017**, (2017)
Q.-H. He, et al., Chinese Phys. C **40**, 114002 (2016)
Q. He, et al., Int. J. Mod. Phys. E. 28, 1950024 (2019)
Q. He, et al., Acta Phys. Pol. B. 51, 463–471 (2020)

BGOegg experiment | Selected physics topics

$\pi^0\pi^0$ correlations

$\pi^0\pi^0$ strong final state interaction through $f_0(500)$ and $f_0(980)$

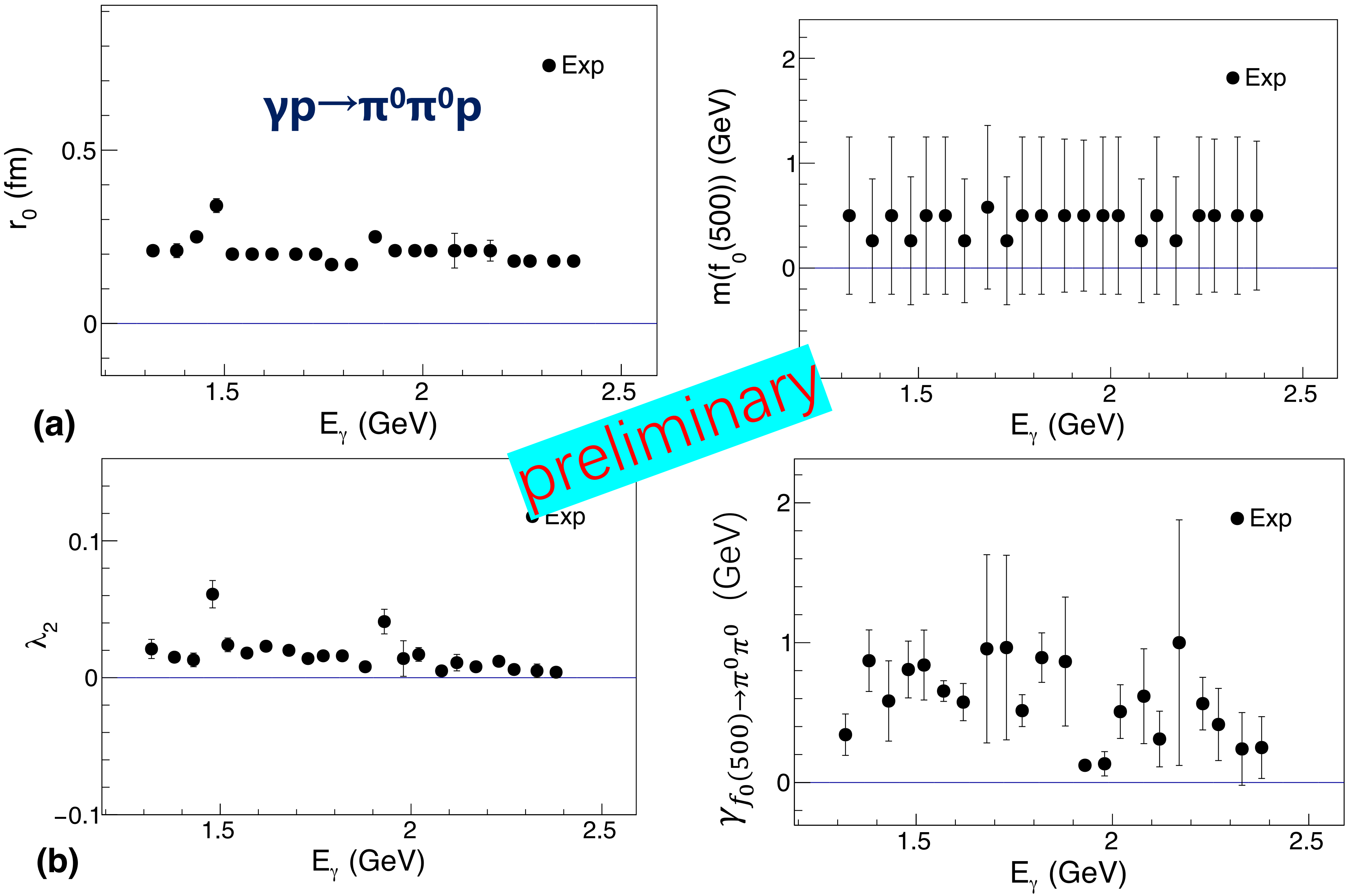

Suppressing $\gamma p \to \pi^0 R \to \pi^0\pi^0 p$ process

R: $\Delta(1232)$, $N(1535)$, $N(1650)$

Free parameters:

$\lambda \in [0,1]$

$R \in$: [0,2] fm

$m(f_0(500)) \in$: [0,1] GeV

$\gamma_{f_0(500)\to\pi^0\pi^0} \in$: [0.1, 1.0] GeV

BGOegg experiment | Selected physics topics

$\pi^0\pi^0$ correlations

$\pi^0\pi^0$ strong final state interaction through $f_0(500)$ and $f_0(980)$

- The preliminary results in case (1) (focusing on Δ) shows the correlation strength is very weak (almost 0) in the beam energy region of 1.3-2.4 GeV.

$\gamma p \rightarrow \pi^0\pi^0 p$

- The preliminary results in case (2) (suppressing $\pi^0\Delta$ or $\pi^0 N^*$ sequential decay) indicate the pi-pi correlations strength decreases as beam energy increases. This phenomenon may be due to the fact that the contribution of the processes ($f_0(500)$ and $f_0(980)$) directly decaying to two pions becomes smaller when the beam energy increases from 1.3 to 2.4 GeV.

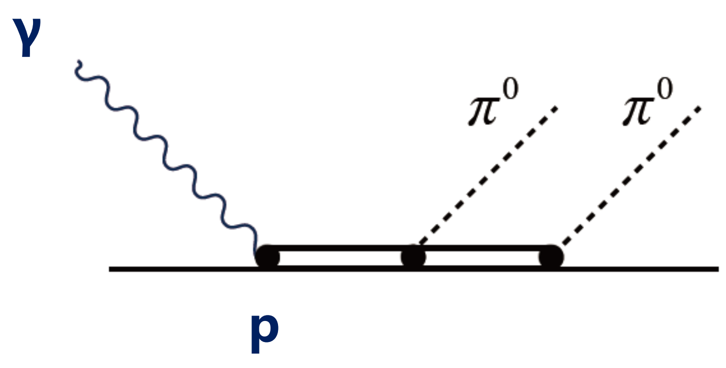

- Including strong final state interaction of $\pi^0\pi^0$ through the $f_0(500)$ and $f_0(980)$ resonance may provide more interesting information

Q. He, The 23rd International Conference on Few-Body Problems in Physics (FB23), Beijing, September 22-27, 2024

Beam asymmetries| Motivation

In meson spectroscopy, more states are found experimentally than are expected from a $q\bar{q}$ scheme. While in baryon spectroscopy, the situation is reverse (missing baryon resonances problem).

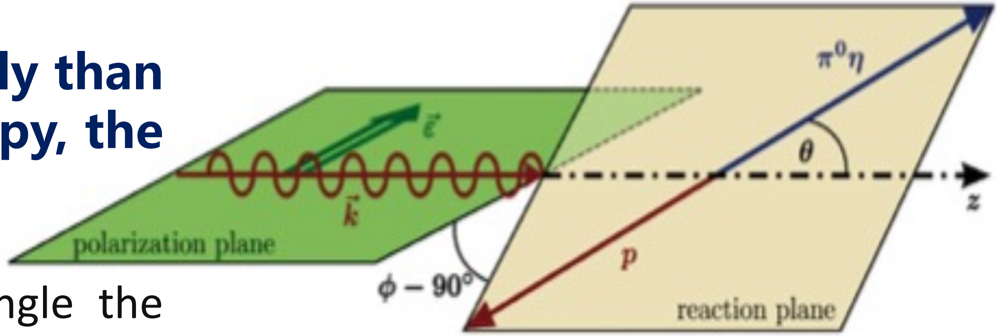

Eur. Phys. J. A (2014) 50: 74

Polarization observables are important in photoproduction to disentangle the multitude of contributing resonances.

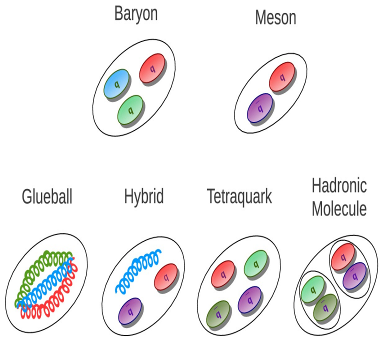

Linearly polarized photons induced photoproduction of single mesons shows a cos 2ϕ dependence. Three body polarization observables I^s, I^c **is highly sensitive** to the dynamics of the reaction (intermediate resonance decay properties).

Baryon resonances can be **generated dynamically from** the interaction of pseudoscalar or vector **mesons** and ground- state octet or decuplet **baryons**.

Three-body dynamics of a **full quark model** or a **quark-diquark** picture (one of the constituent particles of a baryon can be regarded as a quark and the other particle can be considered as a tightly bound state of two quarks, or diquark).

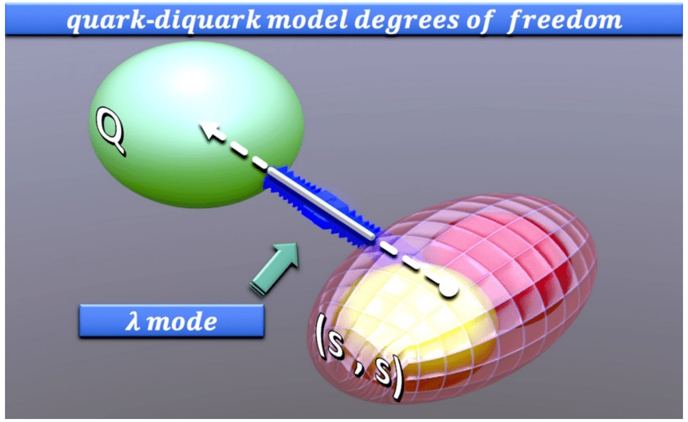

arXiv:1811.01799v2

Beam asymmetries| Motivation

The CBELSA/TAPS Collaboration Eur. Phys. J. A (2014) 50: 74

High statistics study of the reaction $\gamma p \rightarrow p\pi^0\eta$

Abstract. Photoproduction off protons of the $p\pi^0\eta$ three-body final state was studied with the Crystal Barrel/TAPS detector, at the electron stretcher accelerator ELSA in Bonn, for incident energies from the $\pi^0\eta$ production threshold up to 2.5 GeV. Differential cross sections and the total cross sections are presented. The use of linearly polarized photons gives access to the polarization observables Σ, I^s, and I^c, the latter two characterize beam asymmetries in case of three-body final states. $\Delta(1232)\eta$, $N(1535)1/2^-\pi$, and $pa_0(980)$ are the dominant isobars contributing to the reaction. The partial wave analysis confirms the existence of some nucleon and Δ resonances, for which so far only fair evidence was reported. A large number of decay modes of known nucleon and Δ resonances is presented. It is shown that detailed investigations of decay branching ratios may provide a key to unravelling the structure of nucleon and Δ resonances.

Polarized beam energy up to ~1.7 GeV

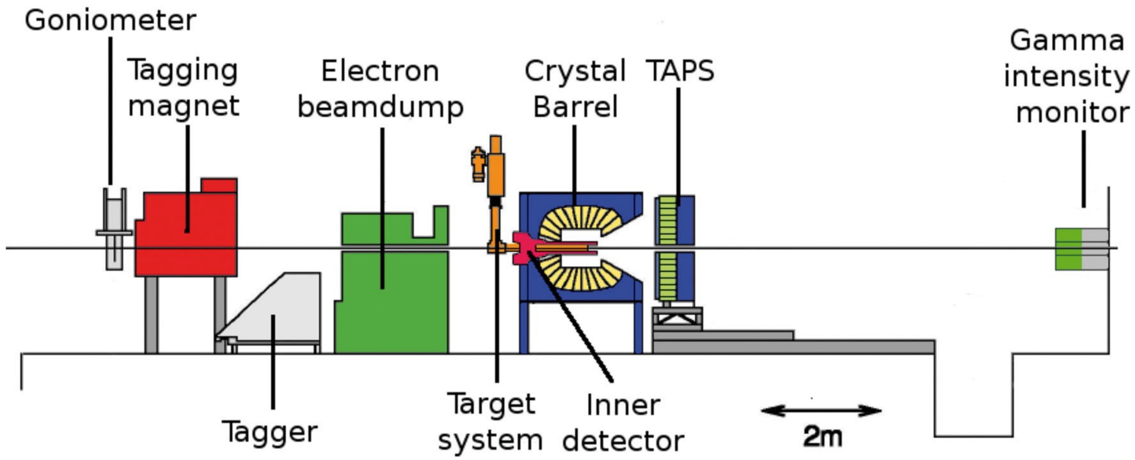

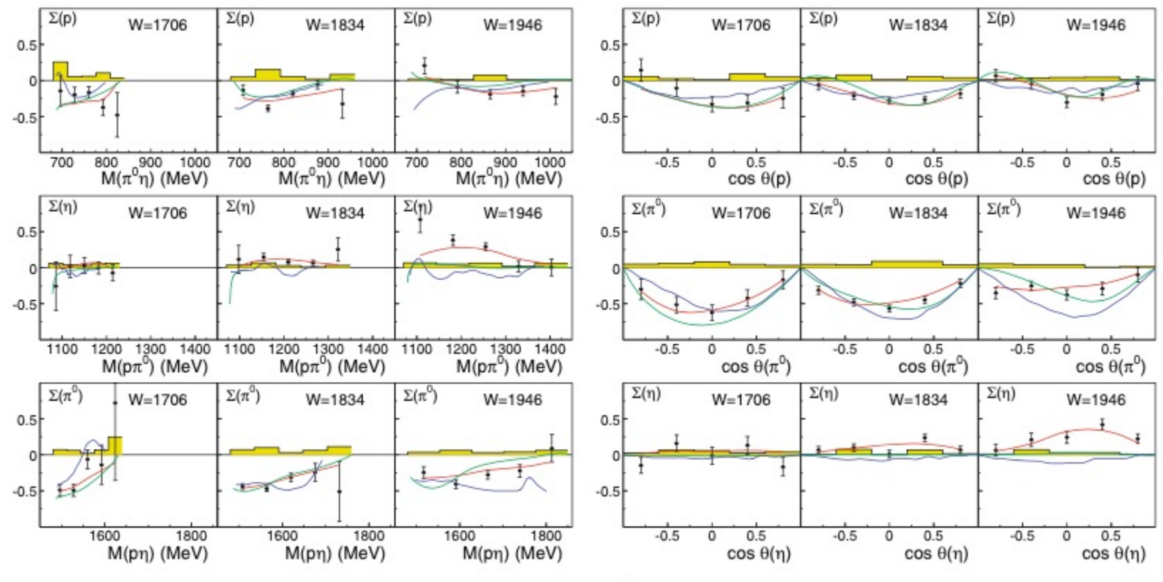

Fig. 31. Two-body beam asymmetry Σ for the reaction $\gamma p \rightarrow p\pi^0\eta$. Top to bottom: incoming photon energy ranges 1085 ± 115 MeV, 1325 ± 125 MeV, 1550 ± 100 MeV. Left: asymmetries obtained from the ϕ distributions of the recoiling (left to right) p, η, π^0 as function of the invariant mass of the other two particles [67]. Right: The same as function of the $\cos\theta$ of the recoiling particle. Systematic error estimate from acceptance studies (yellow). Curves: BnGa-PWA (red), Fix *et al.* [69] (green), Döring *et al.* [50] (blue).

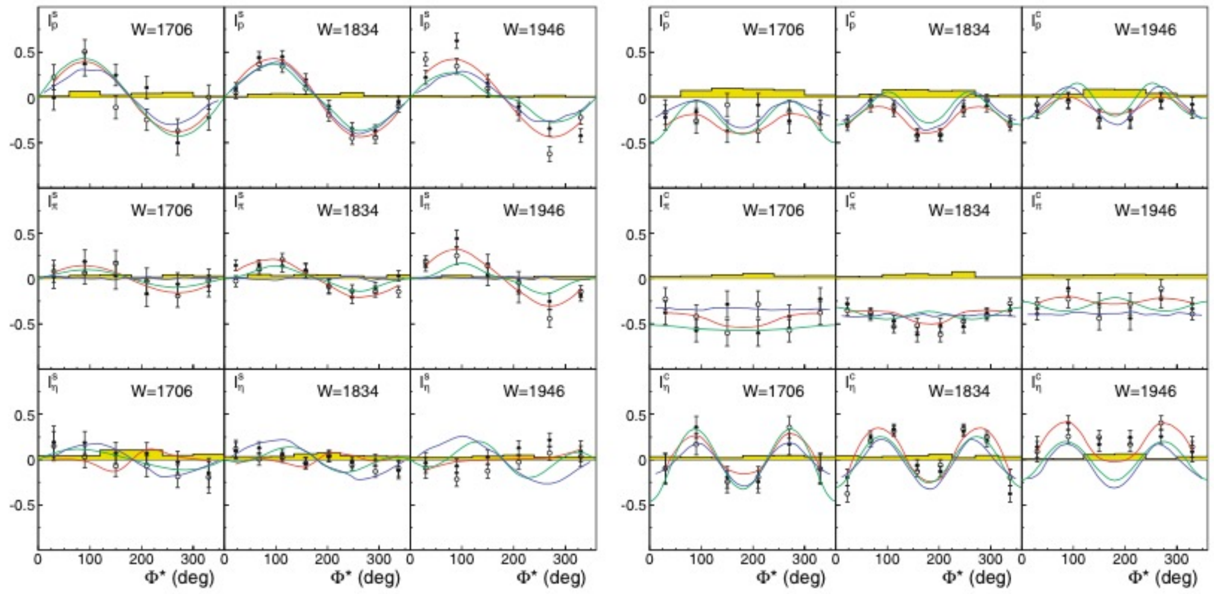

Fig. 32. Three-body beam asymmetries I^s (left) and I^c (right) [49]. Closed symbols: $I^s(\phi^*)$ ($I^c(\phi^*)$) as extracted from the data. Open symbols: $-I^s(2\pi - \phi^*)$, $I^c(2\pi - \phi^*)$ (see eqs. (22) and (23)). Grey bars: systematic error estimate from acceptance studies. Curves: BnGa-PWA (red), Fix *et al.* [69] (green), Döring *et al.* [50] (blue).

$\pi^0\eta$光生反应束流极化度分析

➤ **$\pi^0\eta$光生反应实验**

$$\gamma p \to \pi^0 \eta p \to \gamma\gamma\gamma\gamma p$$

Polarized beam energy up to ~2.4 GeV

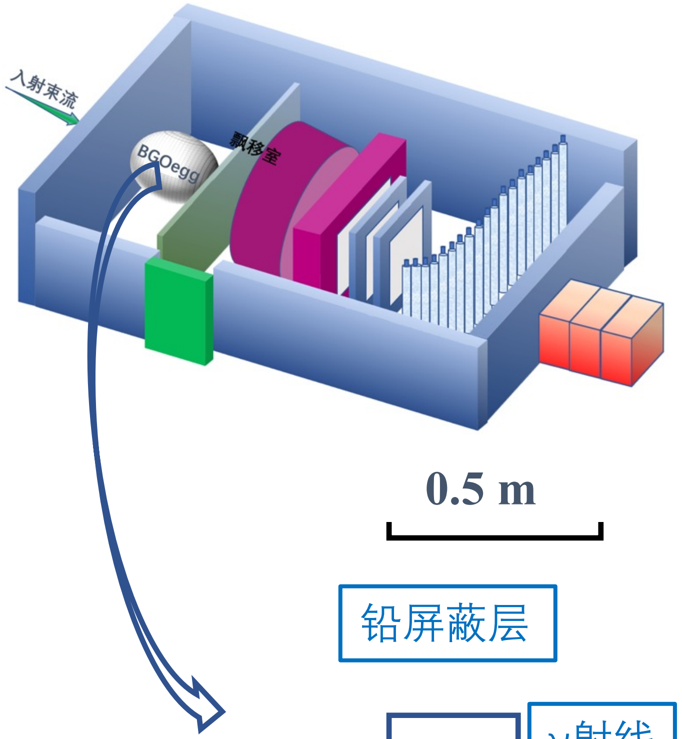

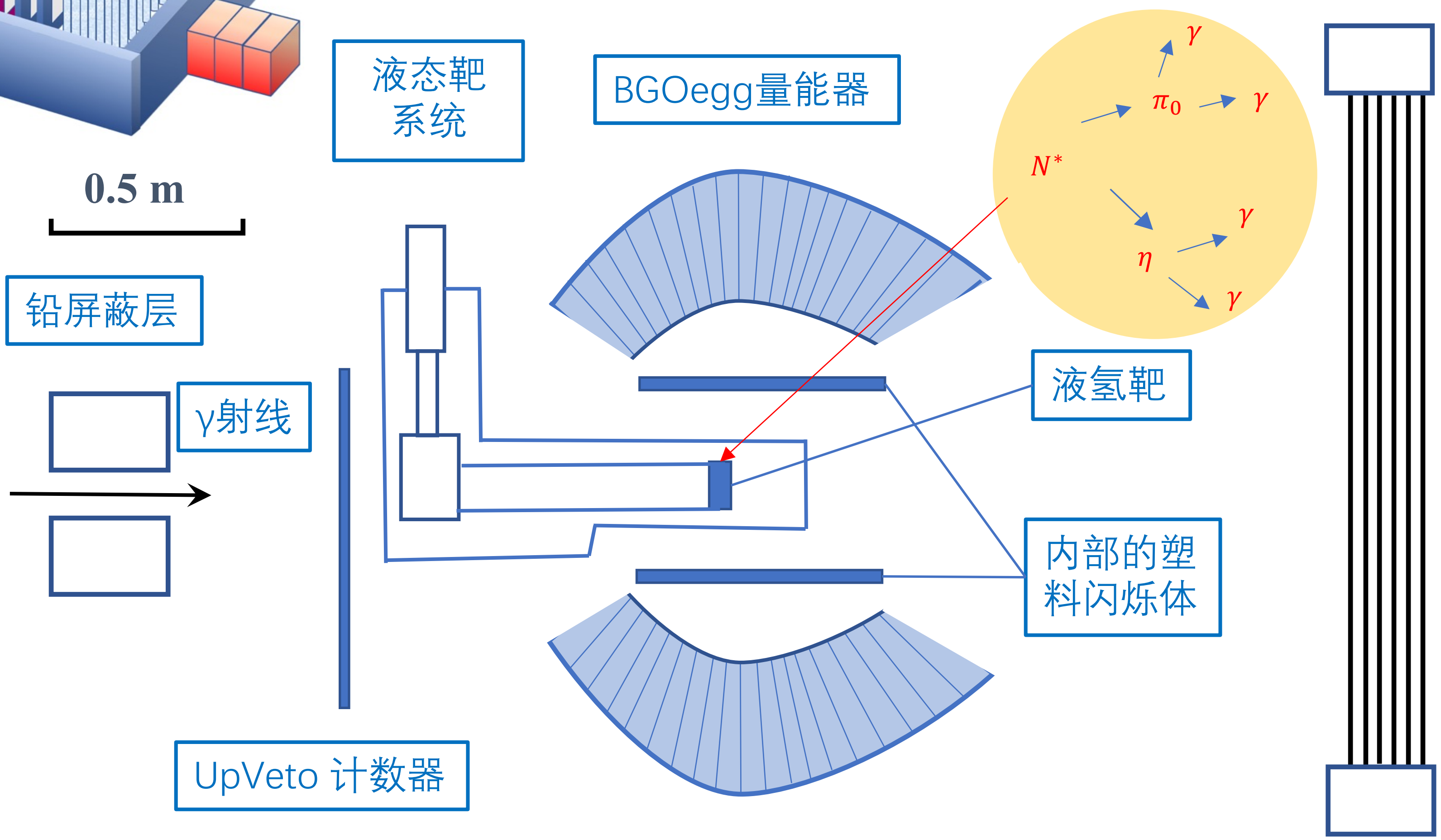

BGOegg

- 1320 BGOcrystals
- Polar coverage: 24°-144°
- EM cluster energy threshold: 30 MeV
- 2 hits $\Delta t < 2$ ns

Planner drift chamber

Polar coverage: $\theta < 21^\circ$

Tagged beam photons

reaches 3.320×10^{12} with the correction for dead times.

4 neutral clusters
1 charged particle hit

Event selection

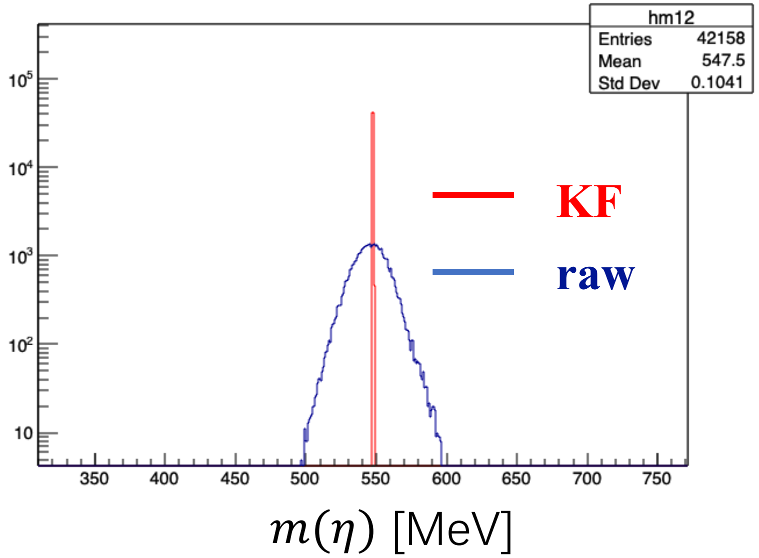

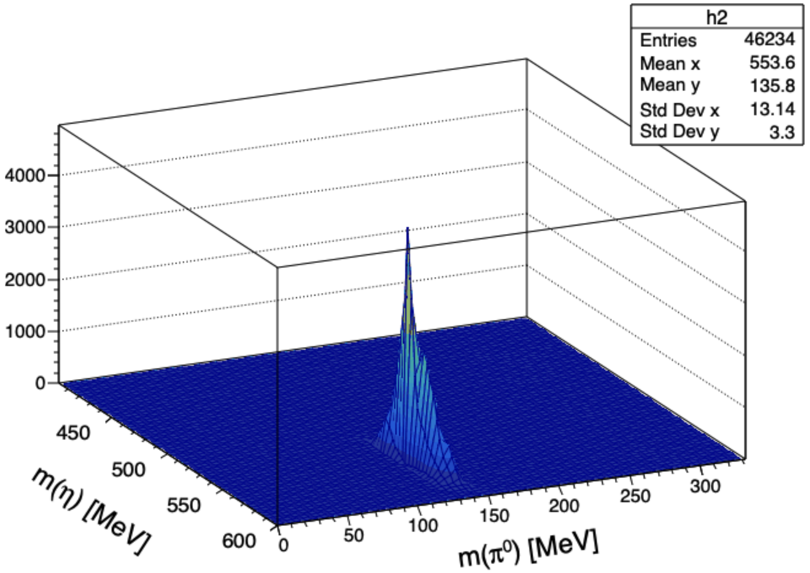

$P(\chi^2)$/ confidence level

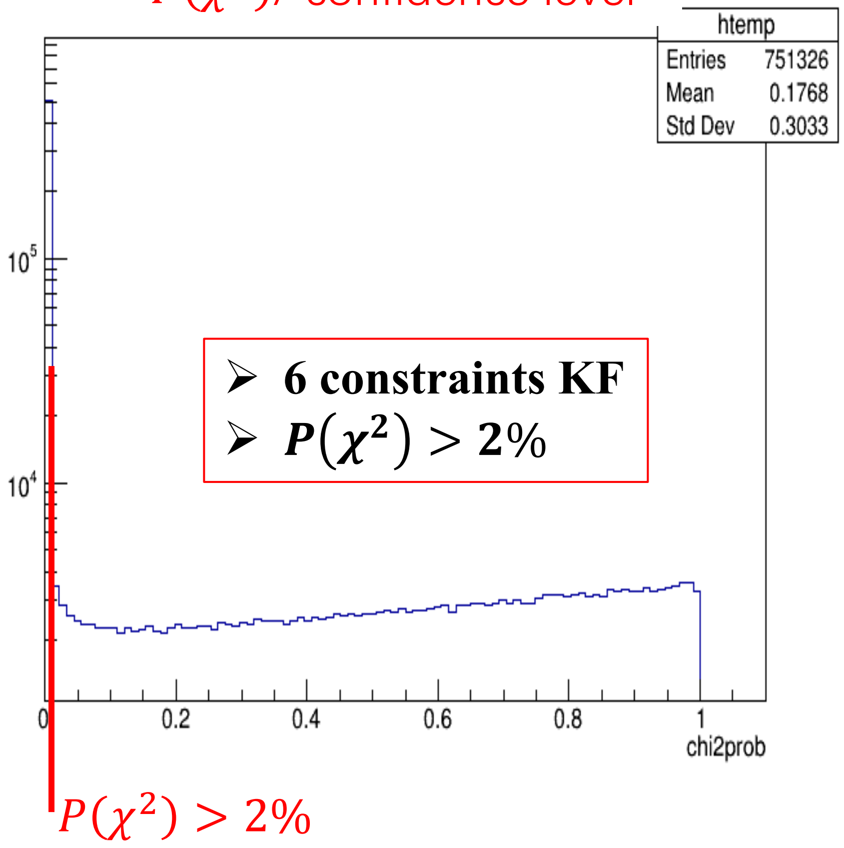

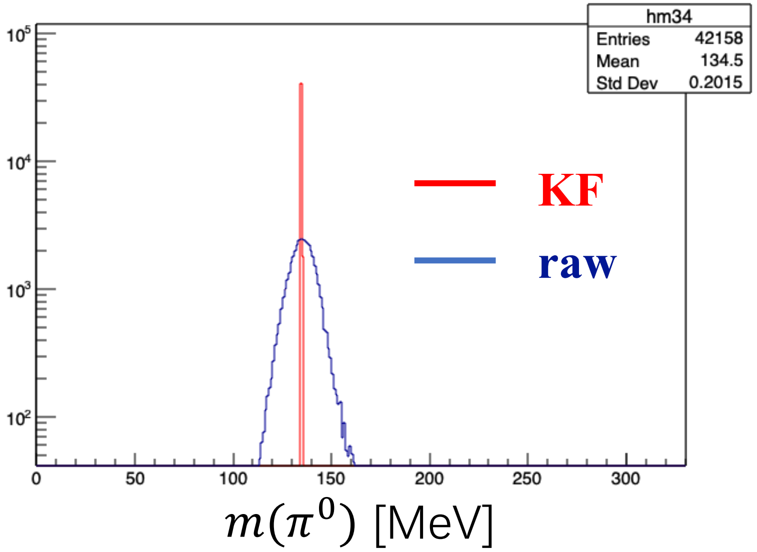

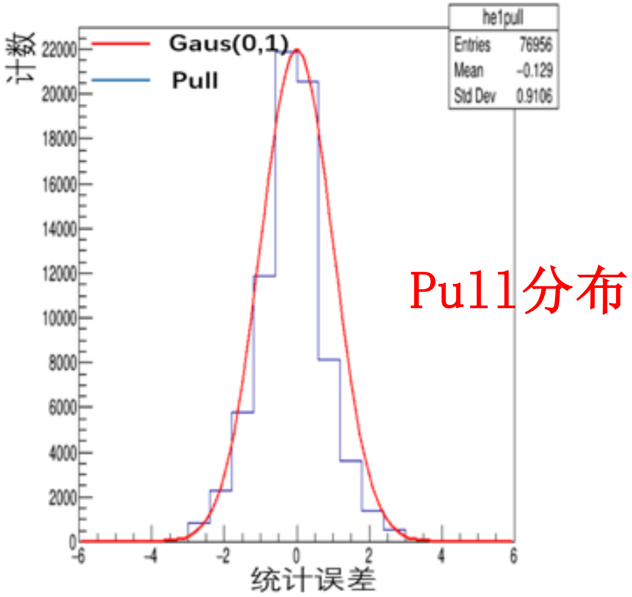

6 constraints:
1-4: 4 momentum conservation
5: invariant mass of η
6: invariant mass of π^0

$\gamma p \to \pi^0 \eta p$ beam asymmetries

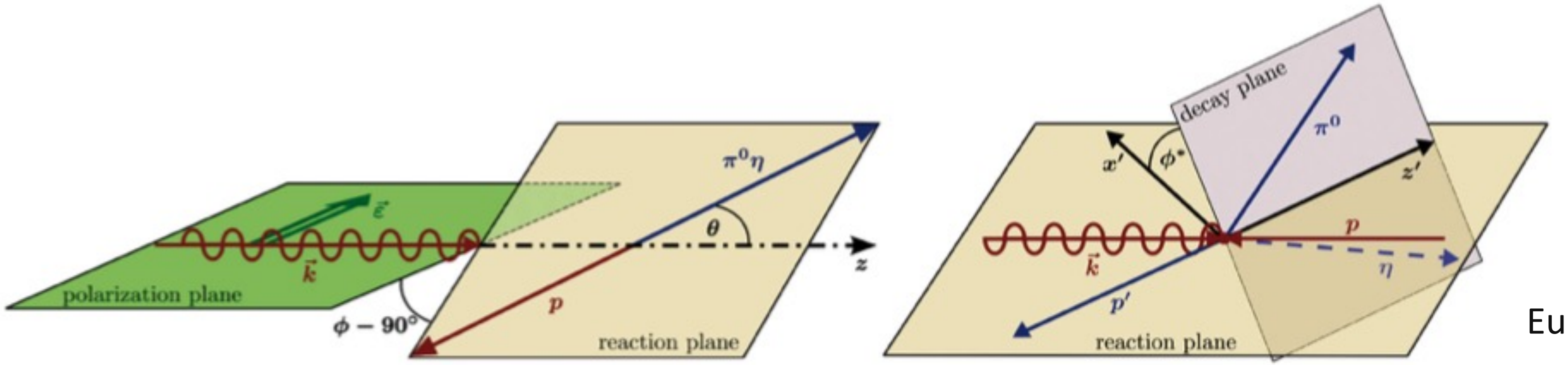

Eur. Phys. J. A (2014) 50: 74

Fig. 29. Angle definitions for the extraction of beam asymmetries. Left: quasi two-body approach. Right: additional degree of freedom occurring in full three-body kinematics.

Quasi two body approach: 1) $\mathbf{p} - (\boldsymbol{\pi^0\eta})$; 2) $\boldsymbol{\pi^0} - (\boldsymbol{\eta}\mathbf{p})$; 3) $\boldsymbol{\eta} - (\boldsymbol{\pi^0}\mathbf{p})$

Cross section $$\frac{d\sigma}{d\Omega} = \left(\frac{d\sigma}{d\Omega}\right)_0 (1 + P\Sigma cos2\phi)$$

P: *degree of polarization of photon beam*

Fit: $f(\phi) = A + P \cdot B \cdot cos2\phi$

Beam Asymmetry: $\Sigma = B/A$

Three-body approach : I^c, I^s

$$\frac{d\sigma}{d\Omega} = \left(\frac{d\sigma}{d\Omega}\right)_0 (1 + P(I^c(\phi^*)cos2\phi + I^s(\phi^*)sin2\phi))$$

Fit: $f(\phi) = A + P(Bcos2\phi + Csin2\phi)$

$I^c(\phi^*) = I^c(2\pi - \phi^*)$ $\quad I^s(\phi^*) = -I^s(2\pi - \phi^*)$

I^c =B/A $\qquad I^s$ = C/A

$\gamma p \to \pi^0 \eta p$ beam asymmetries

$\phi(p)$ binned in $\phi*$

Fit: $f(\phi) = A + P(B\cos 2\phi + C\sin 2\phi)$ I^c:B/A I^s: C/A

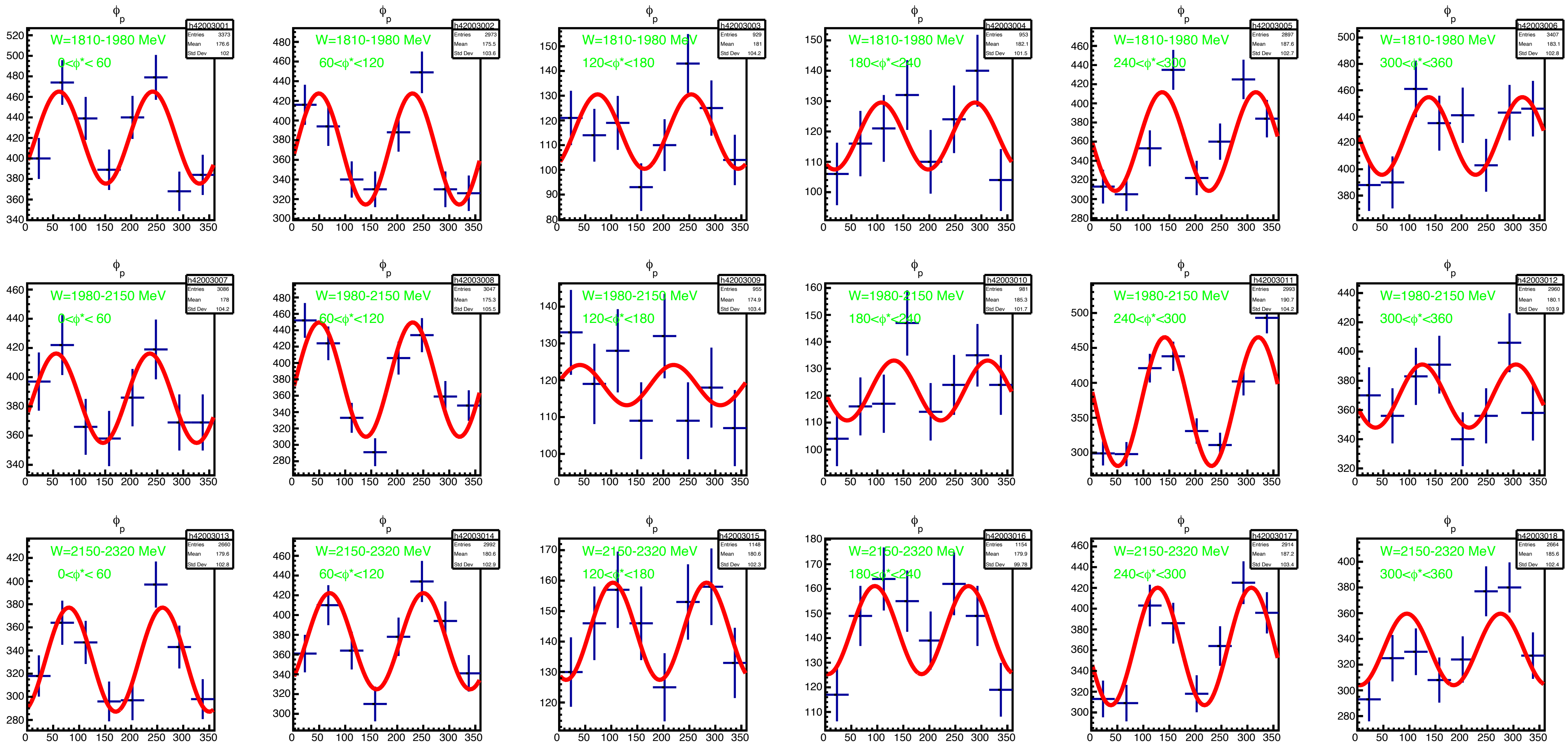

$\gamma p \to \pi^0 \eta p$ beam asymmetries

Σ binned in $cos(\theta_{cm})$

CBELSA: Eur. Phys. J. A (2014) 50: 74

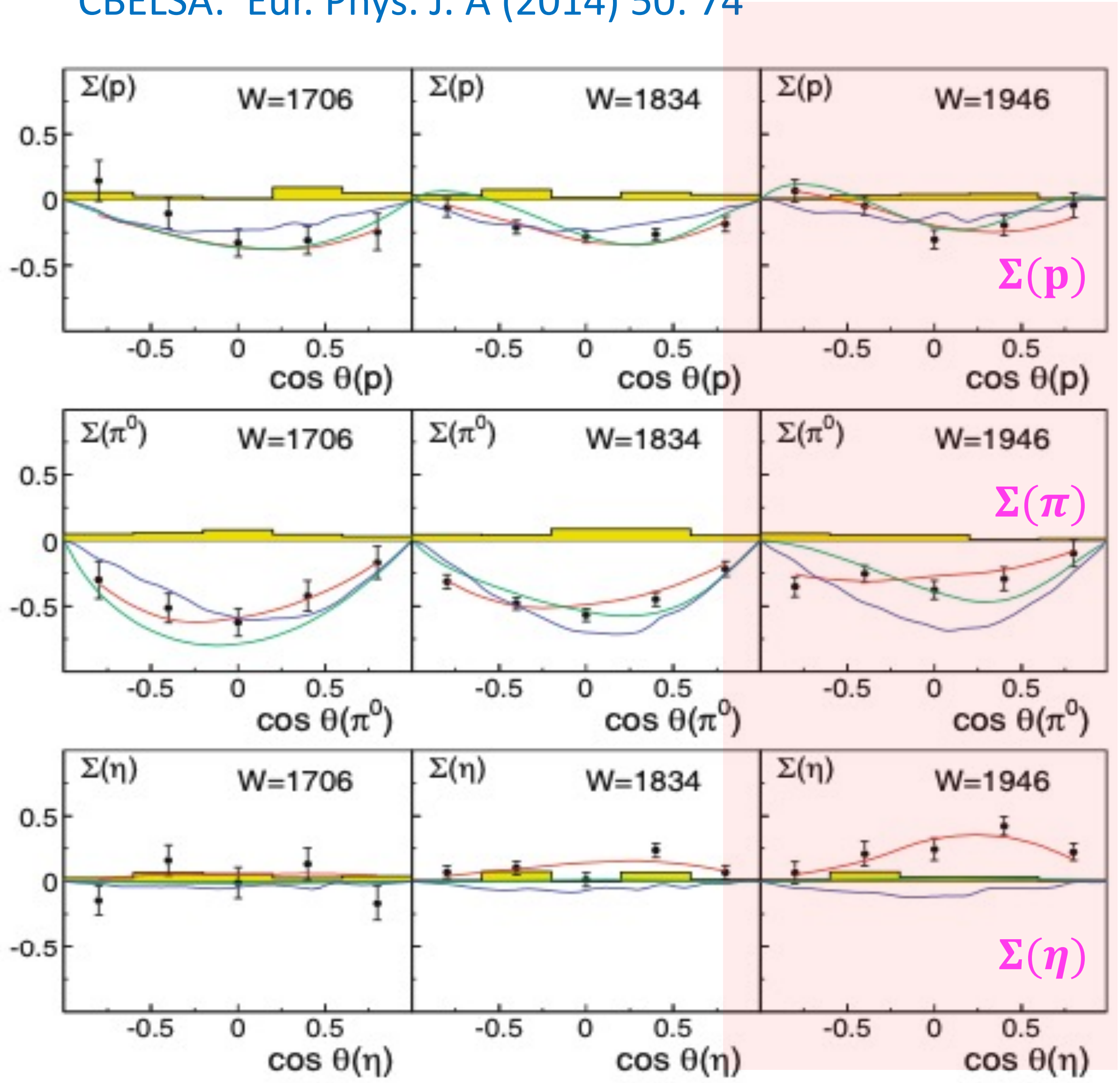

BGOegg 2014B

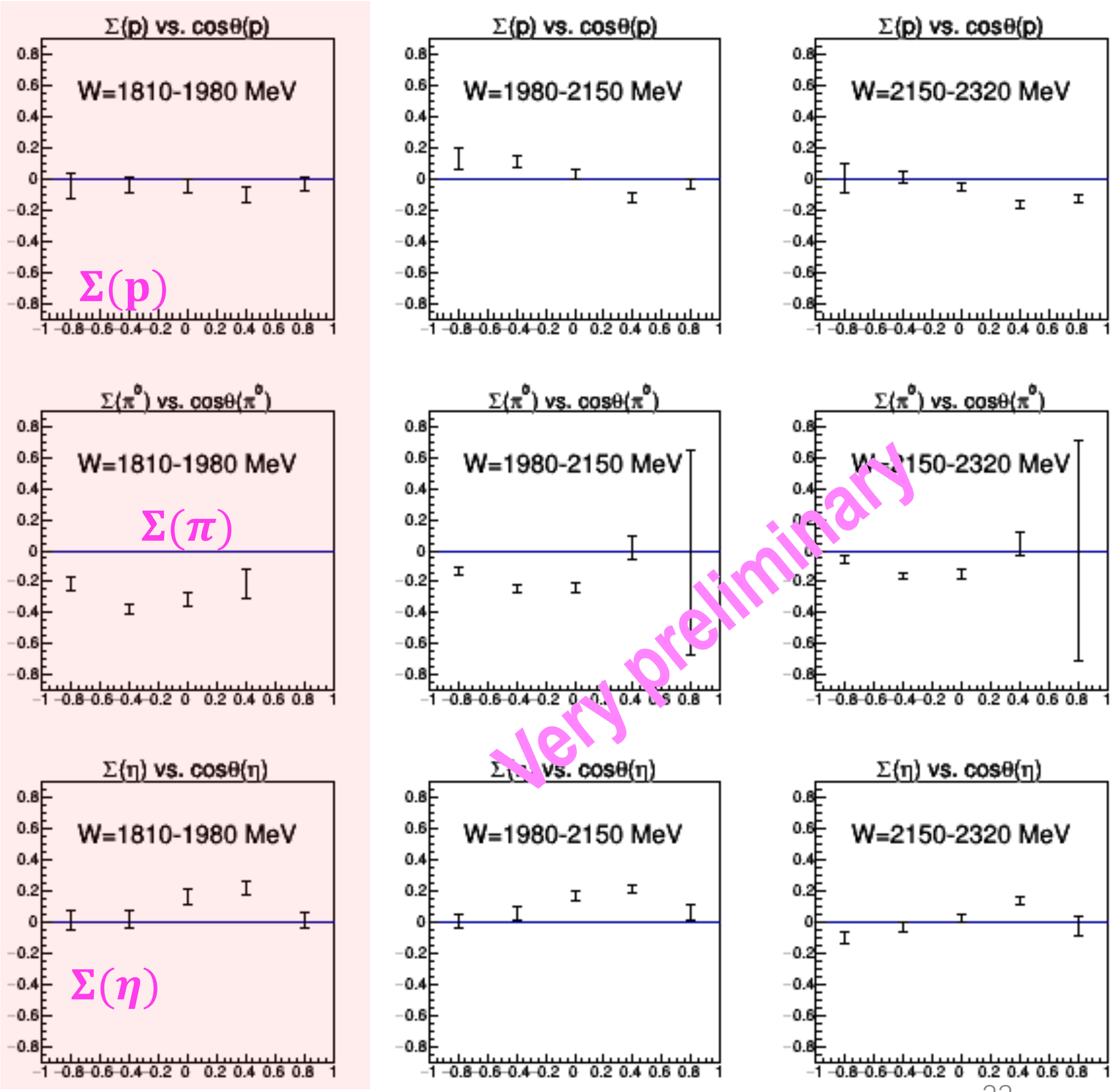

$\gamma p \to \pi^0 \eta p$ beam asymmetries

Σ binned in the invariant mass

CBELSA: Eur. Phys. J. A (2014) 50: 74

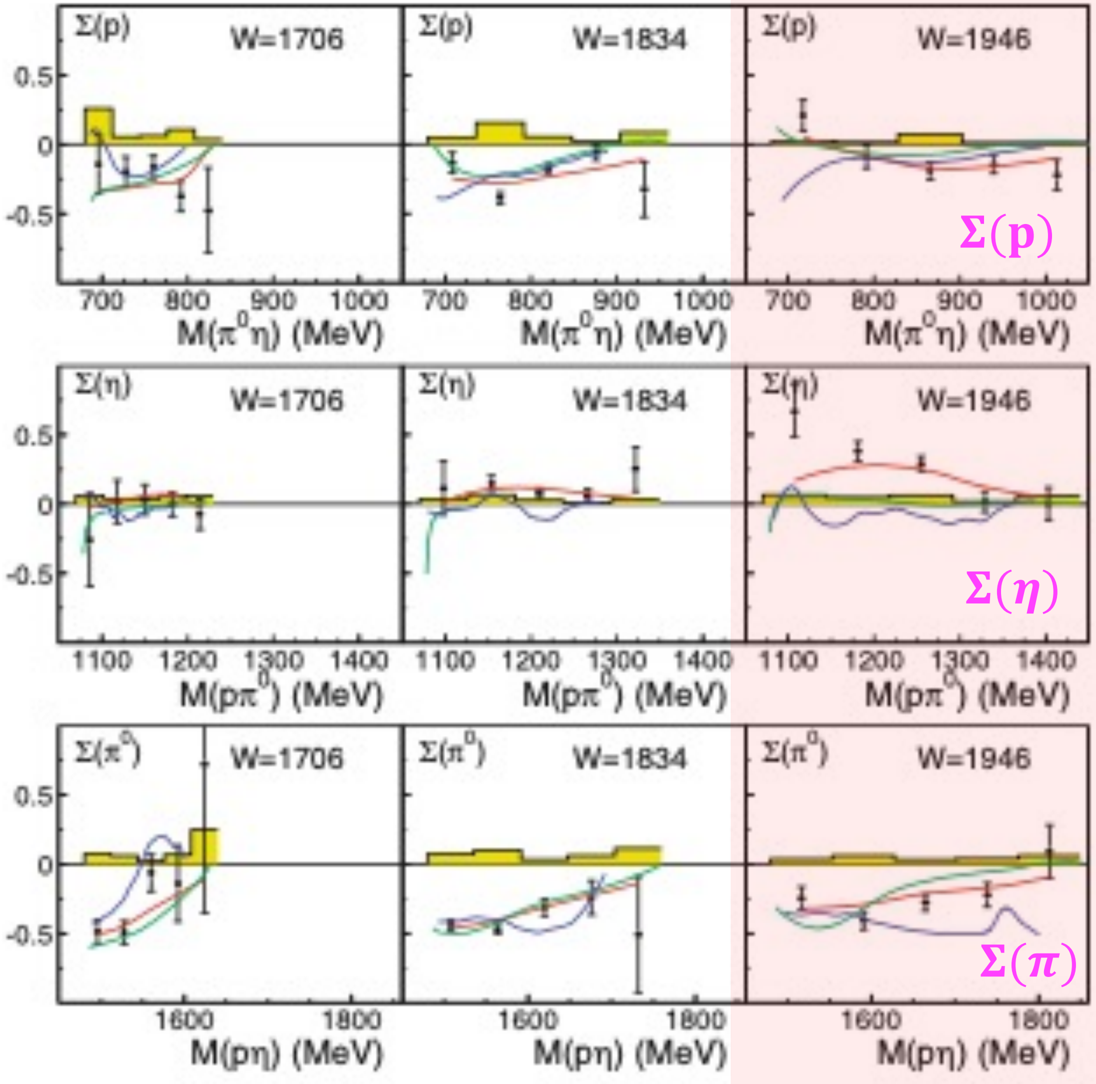

BGOegg 2014B

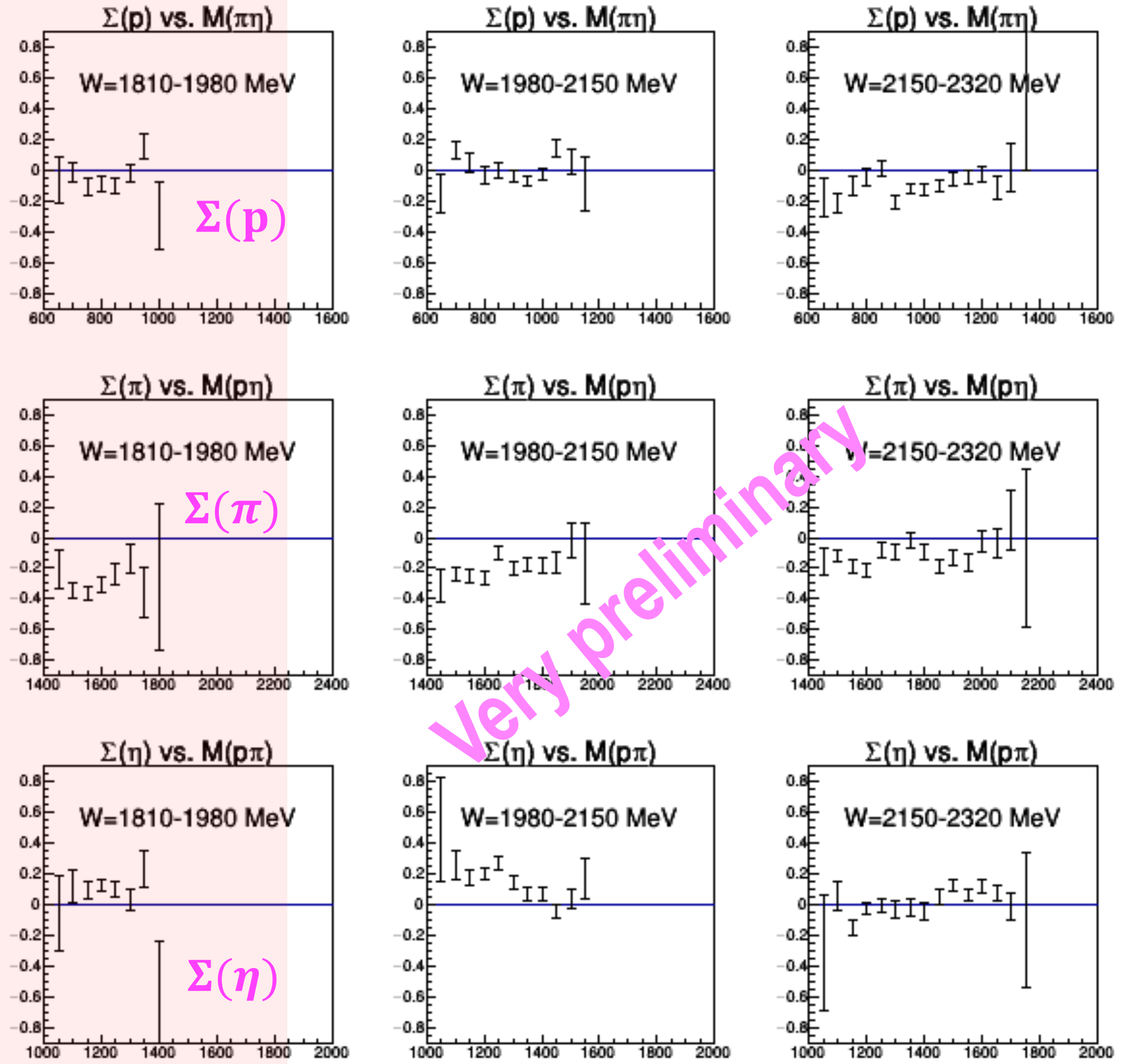

Energy overlap

$\gamma p \rightarrow \pi^0 \eta p$ beam asymmetries

I^c

CBELSA: Eur. Phys. J. A (2014) 50: 74

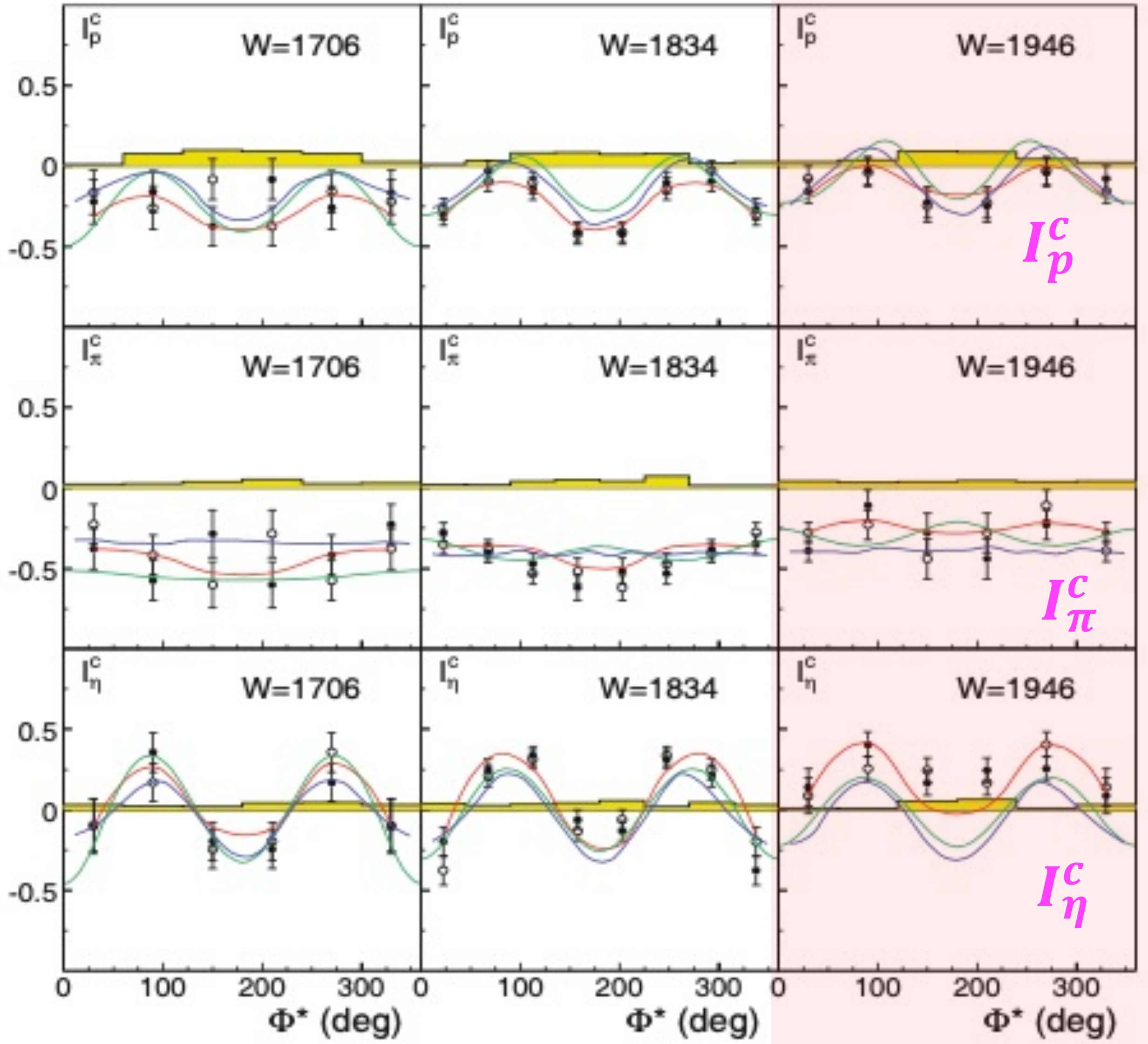

BGOegg 2014B

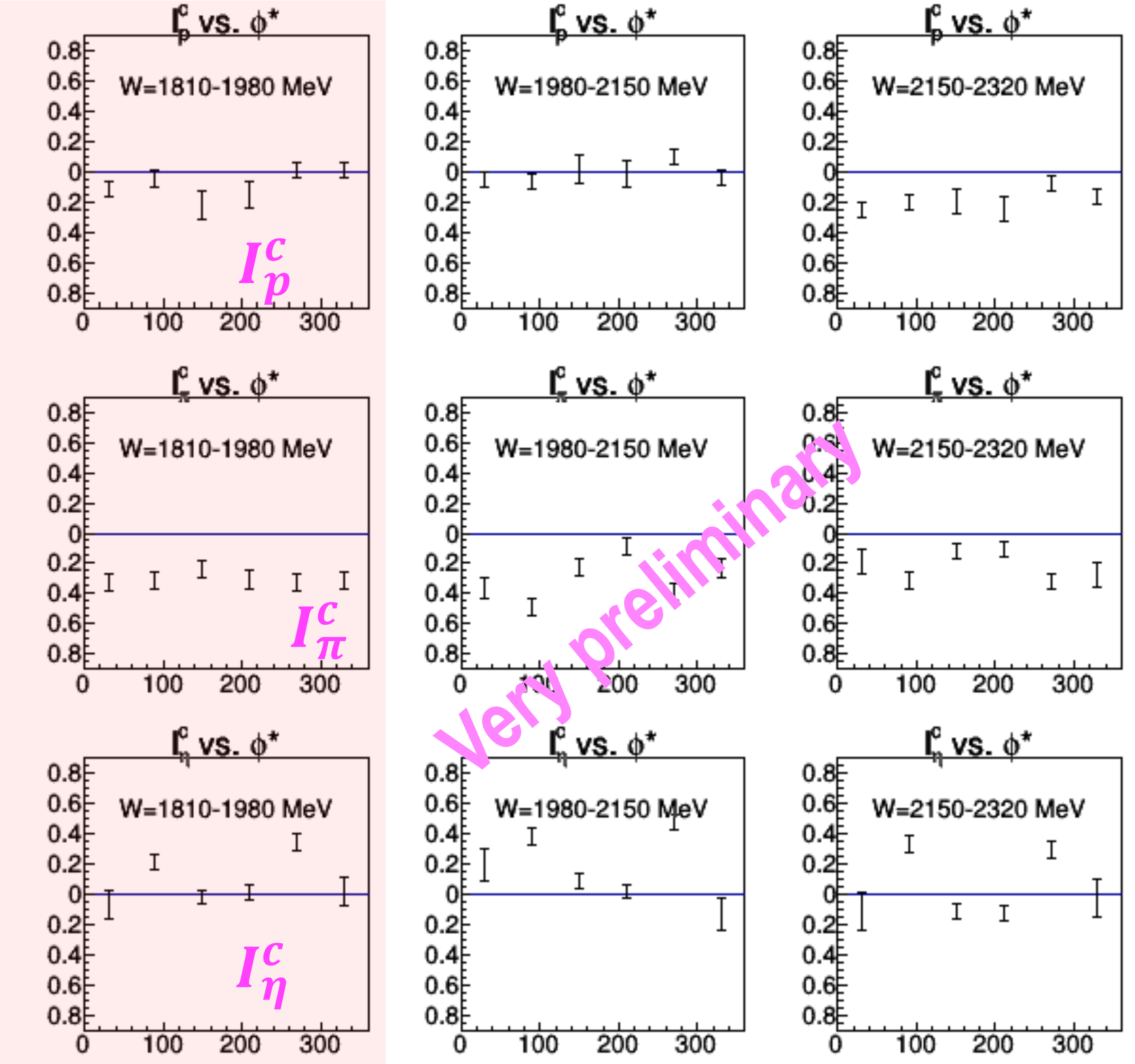

Energy overlap

$\gamma p \rightarrow \pi^0 \eta p$ beam asymmetries

I^s

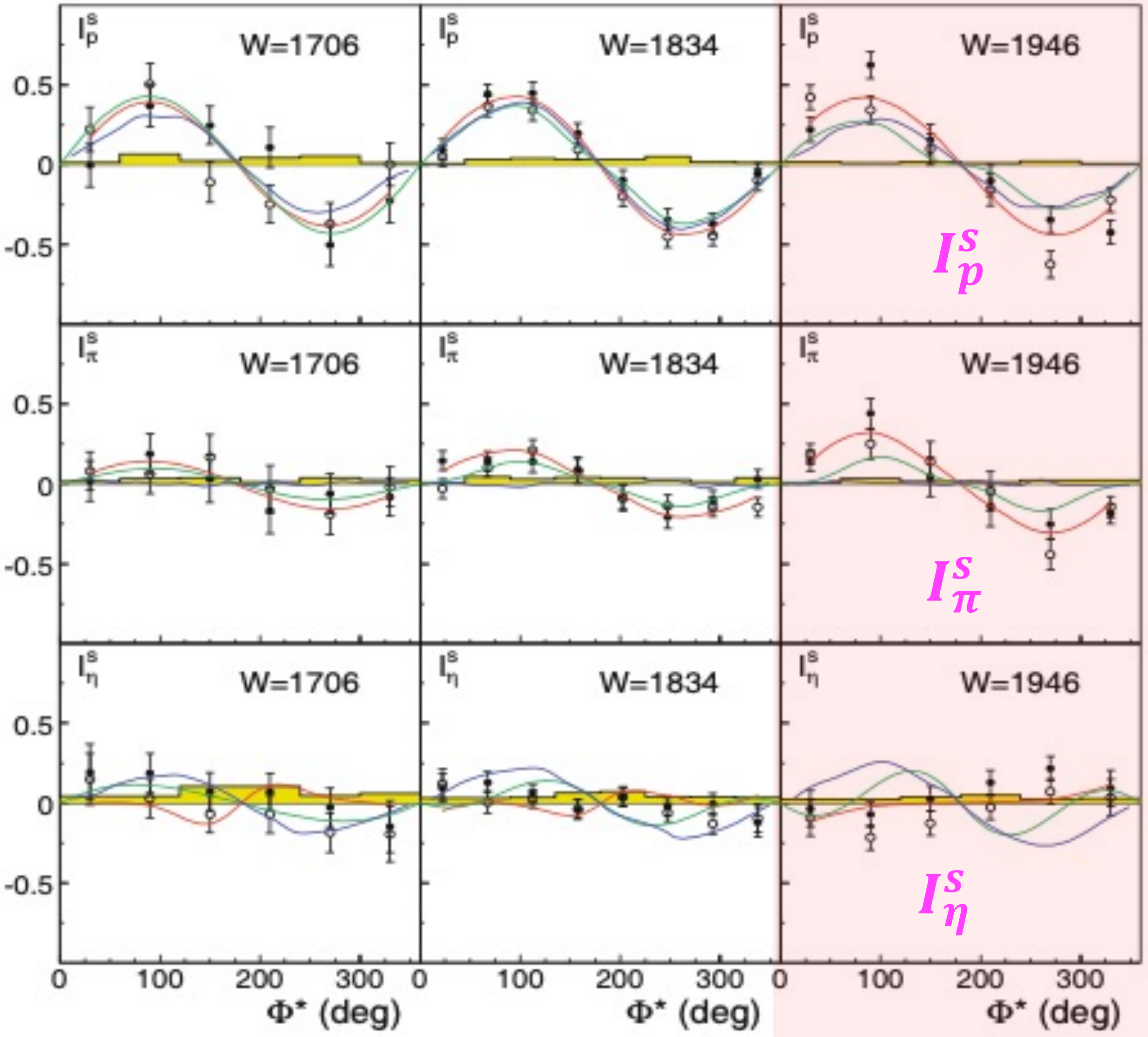

CBELSA: Eur. Phys. J. A (2014) 50: 74

BGOegg 2014B

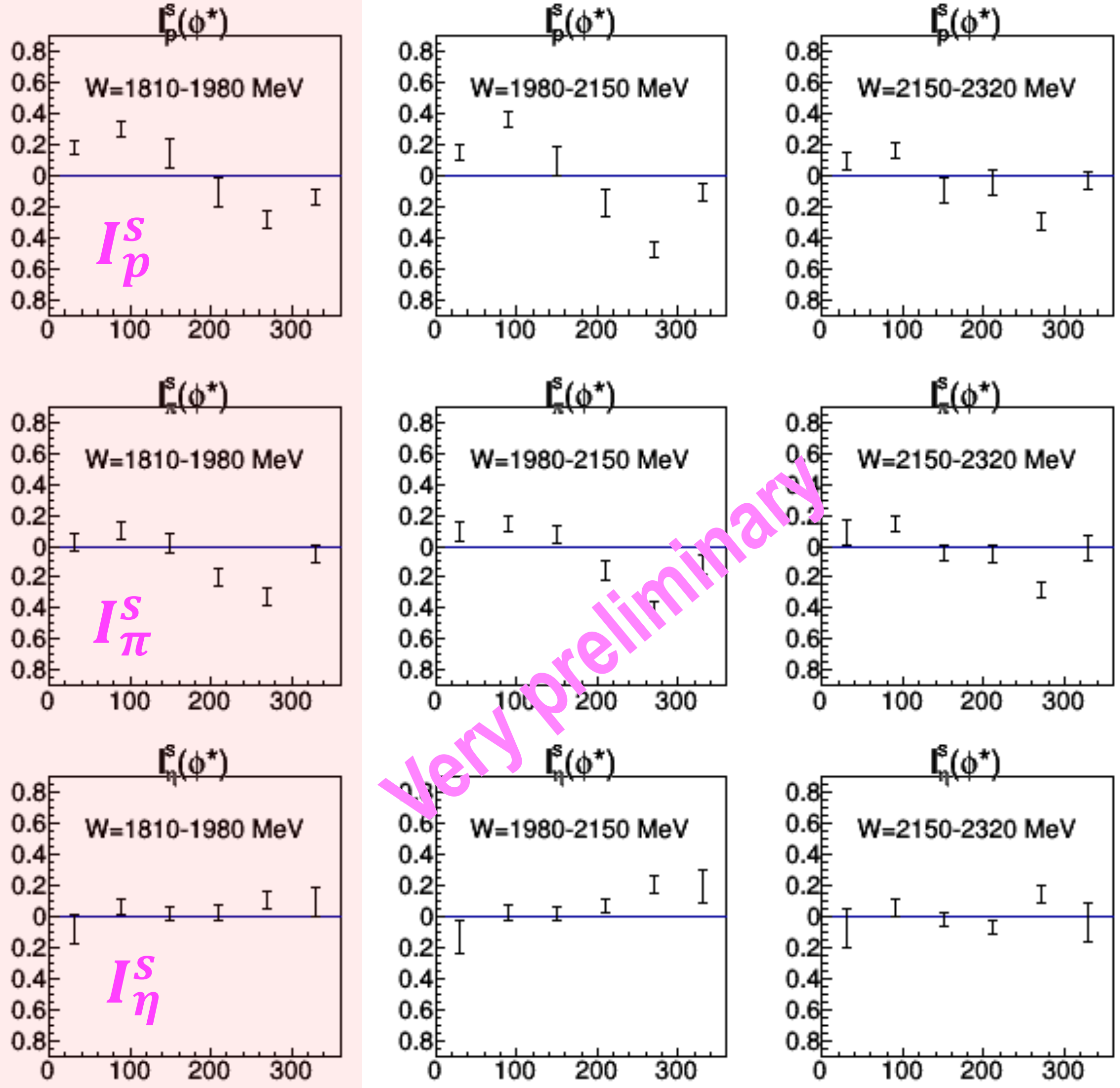

Energy overlap

Discussion

The CBELSA/TAPS Collaboration   Eur. Phys. J. A (2014) 50: 74

Polarized beam energy up to **~1.7 GeV**

Abstract. Photoproduction off protons of the $p\pi^0\eta$ three-body final state was studied with the Crystal Barrel/TAPS detector, at the electron stretcher accelerator ELSA in Bonn, for incident energies from the $\pi^0\eta$ production threshold up to 2.5 GeV. Differential cross sections and the total cross sections are presented. The use of linearly polarized photons gives access to the polarization observables Σ, I^s, and I^c, the latter two characterize beam asymmetries in case of three-body final states. $\Delta(1232)\eta$, $N(1535)1/2^-\pi$, and $pa_0(980)$ are the dominant isobars contributing to the reaction. The partial wave analysis confirms the existence of some nucleon and Δ resonances, for which so far only fair evidence was reported. A large number of decay modes of known nucleon and Δ resonances is presented. It is shown that detailed investigations of decay branching ratios may provide a key to unravelling the structure of nucleon and Δ resonances.

Table 3. Branching ratios of nucleon and Δ resonances.

Resonance	πN	$N(1535)\pi$	$\Delta(1232)\eta$
$N(1710)1/2^+$	$5 \pm 3\%$	$15 \pm 6\%$	–
$N(1880)1/2^+$	$6 \pm 3\%$	$8 \pm 4\%$	–
$N(1900)3/2^+$	$3 \pm 3\%$	$7 \pm 3\%$	–
$N(2100)1/2^+$	$3 \pm 2\%$	$22 \pm 8\%$	–
$N(2120)3/2^-$	$5 \pm 3\%$	$15 \pm 8\%$	–
$\Delta(1700)3/2^-$	$22 \pm 4\%$	$1 \pm 0.5\%$	$5 \pm 2\%$
$\Delta(1900)1/2^-$	$7 \pm 2\%$	–	$1 \pm 1\%$
$\Delta(1905)5/2^+$	$13 \pm 2\%$	$\leq 1\%$	$4 \pm 2\%$
$\Delta(1910)1/2^+$	$12 \pm 3\%$	$5 \pm 3\%$	$9 \pm 4\%$
$\Delta(1920)3/2^+$	$8 \pm 4\%$	$\leq 2\%$	$11 \pm 6\%$
$\Delta(1940)3/2^-$	$2 \pm 1\%$	$8 \pm 6\%$	$10 \pm 6\%$
$\Delta(1950)7/2^+$	$46 \pm 2\%$		$\leq 1\%$

$N(1710)1/2^+$ ***

$N(1710)1/2^+$ pole parameters			
M_{pole}	1690 ± 15	Γ_{pole}	170 ± 20
$A^{1/2}$	0.052 ± 0.014	Phase:	$(-10 \pm 50)^\circ$
$N(1710)1/2^+$ transition residues			phase
$\pi N \to \pi N$		6 ± 3 (MeV)	$(120 \pm 45)^\circ$
$2(\pi N \to N(1535)\pi)/\Gamma$		$10 \pm 4\%$	$(140 \pm 40)^\circ$
$(\gamma p)^{1/2} \to N(1535)\pi$	M_{1-}	$8.5 \pm 3.5\ 10^{-3}$	$(25 \pm 35)^\circ$
$N(1710)1/2^+$ Breit-Wigner parameters			
M_{BW}	1715 ± 20	Γ_{BW}	175 ± 15
$\text{Br}(\pi N)$	$5 \pm 3\%$	$\text{Br}(N(1535)\pi)$	$15 \pm 6\%$
$A^{1/2}_{BW}$	0.050 ± 0.010		

BGOegg 2014B

Polarized beam energy up to ~2.4 GeV

(1) cascade processes of higher mass resonances into a resonance with intrinsic orbital angular momentum can be studied

(2) The comparison of these decay modes with decays into Nπ is very helpful for identifying mechanisms responsible for the decays of N and Δ resonances.

(3) More information about branching ratios for decays into Nπ, N(1535)π, and Δ(1232)η can be obtained.

Summary

- Preliminary results of beam asymmetries of $\gamma p \to \pi^0 \eta p$ in the beam energy region of 1.3-2.4 GeV were obtained.
- The quasi 2-body polarization observables Σ and 3-body observables I^s, I^c above ~1.7 GeV (E_γ) are new experimental data in the world.
- Our results are consistent with CBELSA's results in the beam energy region of 1.3-1.7 GeV within error bars
- Systematic uncertainties estimation is currently underway
- Cooperation with PWA could provide more interesting information about cascade processes of higher mass resonances and branching ratios for decays into Nπ, N(1535)π, and Δ(1232)η

Acknowledgements

Norihito Muramatsu
IMP

Hajime Shimizu
Tohoku University

M. Miyabe
Tohoku University

H. Yamazaki
Tohoku University

Atsushi Tokiyasu
Tohoku University

Toshikazu Hashimoto
Osaka University

Takatsugu Ishikawa
Osaka University

Tianzhu MO
NUAA

Shengkai WANG
NUAA

Thanks